

TA 7

C6

CER 69/70-23

copy 2

C. E. - R. R. 69/70

Project THEMIS
Technical Report No. 6

FLOW SEPARATION IN TIME VARYING FLOW

by

Fang-Kuo Chou

and

V. A. Sandborn



ENGINEERING RESEARCH

AUG 18 1970

FOOTHILLS READING ROOM

**FLUID MECHANICS PROGRAM
ENGINEERING RESEARCH CENTER
COLLEGE OF ENGINEERING
COLORADO STATE UNIVERSITY
FORT COLLINS, COLORADO**

ABSTRACT

An exact solution of time varying pipe flow with a fluctuating velocity superimposed on the mean flow is analyzed. The velocity profiles, together with the profile parameters at separation, are computed from a computer program.

The results are compared with the model for relaxed (steady) and unrelaxed (unsteady) separation criteria proposed by V. A. Sandborn and S. J. Kline. For very low frequencies, the correlation curves appear to have a reasonable agreement with the proposed relaxed separation criterion. For high frequencies, the correlation curves have been found to fall approximately on the unrelaxed separation criterion. This result demonstrates further that adjustment time is an important factor for separation to be relaxed or unrelaxed, a new concept proposed by Sandborn.

In addition, J. T. Stuart's solution for the flow along an infinite flat plate with normal suction and periodic external velocity is further analyzed. The results again prove to agree with the proposed new concept.

TABLE OF CONTENTS

<u>Chapter</u>	<u>Page</u>
	LIST OF TABLES v
	LIST OF FIGURES. vi
	LIST OF SYMBOLS. viii
I	INTRODUCTION 1
II	REVIEW OF LITERATURE 4
	2.1 Introduction. 4
	2.2 Lighthill's Theory of the Response of Skin Friction to Fluctuations in the Stream Velocity 6
	2.3 Fluctuating Flow Past an Infinite Flat Plate with Suction. 7
	2.4 Unsteady Flow Through Pipe. 8
III	ANALYSIS OF UNSTEADY PIPE FLOW SEPARATION AND SEPARATION IN FLUCTUATING FLOW PAST A POROUS FLAT PLATE 10
	3.1 Unsteady Pipe Flow. 10
	3.1.1 Solution of unsteady pipe flow 10
	3.1.2 Velocity distributions and velocity profile parameters at separation 14
	3.1.3 Comparison with the relaxed and unrelaxed separation correlations. 20
	3.2 Fluctuating Flow Past a Porous Flat Plate 25
	3.2.1 Velocity distributions and velocity profile parameters at separation 25
	3.2.2 Comparison with the relaxed and unrelaxed separation correlations. 34
IV	CONCLUDING REMARKS 41
	BIBLIOGRAPHY 43

LIST OF TABLES

<u>Table</u>		<u>Page</u>
1	VARIATIONS WITH X OF $BER X$, $BEI X$, $BER'X$, $BEI'X$ FROM $X=0$ TO $X=80$	47
2	VARIATIONS OF δ^*/R , θ/R , H , AND ϵ WITH RESPECT TO $\sqrt{\frac{\omega}{\nu}} R$ FOR TIME VARYING PIPE FLOW.	49
3	VARIATIONS OF SEPARATION PROFILE PARAMETERS FOR FLUCTUATING FLOW PAST A POROUS FLAT PLATE.	51

LIST OF FIGURES

<u>Figure</u>		<u>Page</u>
1	Relaxed and unrelaxed separation correlations	5
2	Plots showing the functions $\text{Ber } x$, $\text{Bei } x$, $\text{Ber}' x$, $\text{Bei}' x$	13
3(a-c)	Velocity profiles at separation for time varying pipe flow	16-18
4	Comparison of the high frequency separation profile with the velocity profile for steady flow, and the low frequency separation profile with the relaxed separation profile of Eq. (2-2).	19
5	Some particular types of separation profiles in time varying pipe flow calculated from Eq. (3-13)	21
6	Variations of ϵ with respect to $\sqrt{\frac{\omega}{\nu}} R$ for time varying pipe flow at separation	22
7	Comparison of time varying pipe flow separation profile parameters with the empirical relaxed and unrelaxed separation correlations for various ωt 's.	24
8	Variations of the form factor at separation with the pressure gradient parameter $\frac{R^2}{\nu} \frac{1}{U} \frac{dU}{dt}$ for time varying pipe flow	26
9	Variations of the form factor at separation with the pressure gradient parameter $\frac{\theta^2}{\nu} \frac{1}{U} \frac{dU}{dt}$ for time varying pipe flow	27
10(a-e)	Variations of ϵ and U/U_0 at separation with respect to λ for fluctuating flow past a porous flat plate.	29,30
11(a-c)	Velocity profiles at separation for fluctuating flow past a porous flat plate	31-33
12	Comparison of separation profile parameters of fluctuating flow past a porous flat plate with the empirical relaxed and unrelaxed separation correlations.	35
13(a-b)	Separation velocity profiles for the points on the hooks	37,38

LIST OF FIGURES - Continued

<u>Figure</u>		<u>Page</u>
14	Variations of the form factor at separation with the pressure gradient parameter $\frac{\delta^2}{\nu} \frac{1}{U} \frac{dU}{dt}$ for fluctuating flow past a porous flat plate	39
15	Variations of the form factor at separation with the pressure gradient parameter $\frac{\theta^2}{\nu} \frac{1}{U} \frac{dU}{dt}$ for fluctuating flow past a porous flat plate	40

LIST OF SYMBOLS

<u>Symbol</u>	<u>Definition</u>
C	Constant
H	Velocity form factor
J_0	Bessel function of the first kind and zeroth order
K	Constant
m	Constant
P	Static pressure
R	Radius of pipe
r	Radial distance from the axis of pipe
t	Time scale
U	Free stream velocity or velocity in the axis of pipe
U_0	Mean of U
u	Velocity in x-direction
u_0	Mean of u
v	Velocity in y-direction
v_0	Mean of v
v_w	Constant velocity component normal to the wall
x	Coordinate parallel to wall or to the axis of pipe
y	Coordinate normal to wall
α	Phase lead
δ	Boundary layer thickness
δ^*	Displacement thickness
δ_0^*	Displacement thickness of the unperturbed boundary layer
ϵ	Constant

LIST OF SYMBOLS - Continued

<u>Symbol</u>	<u>Definition</u>
ϵU_0	Amplitude of free stream velocity fluctuation or of velocity fluctuation in the axis of pipe
ϵu_1	Amplitude of velocity fluctuation in x-direction
ϵv_1	Amplitude of velocity fluctuation in y-direction
η	Non-dimensional variable $y v_w /\nu$
η_1	Non-dimensional variable y/δ
$\zeta_0(y)U_0$	Mean velocity in x-direction
$\zeta_1(y)\epsilon U_0$	Amplitude of velocity fluctuation in x-direction
θ	Momentum thickness
λ	Frequency parameter $\omega\nu/v_w^2 = \omega\delta_0^{*2}/\nu$
λ_t	Pressure parameter in unsteady flow $-\frac{R^2}{\nu} \frac{1}{U} \frac{dU}{dt}$ or $-\frac{\delta^2}{\nu} \frac{1}{U} \frac{dU}{dt}$
λ_δ	Pohlhausen pressure parameter $-\frac{\delta^2}{\nu} \frac{dU}{dx}$
λ_θ	Pressure parameter in unsteady flow $-\frac{\theta^2}{\nu} \frac{1}{U} \frac{dU}{dt}$
μ	Absolute viscosity
ν	Kinematic viscosity
ρ	Density
τ_0	Unperturbed wall shear stress
τ_w	Shear stress at wall
ω	Frequency (rad/s)
ω_0	Critical frequency
Suffixes	
w	Denotes value evaluated at the wall
s	Denotes value of quasi-steady solution

Chapter I

INTRODUCTION

The problem of boundary layer separation has become very important in recent times, especially, in the field of aeronautics; in actual applications it is often necessary to prevent separation in order to reduce drag and to attain high lift.

A model classifying boundary layer separation, either laminar or turbulent, as relaxed (steady) and unrelaxed (unsteady) was first proposed by Sandborn and Kline (13). The proposed model was further demonstrated both theoretically and experimentally by Liu (6). The relaxed boundary layer separation was defined as the point or line where shear stress at the wall vanishes continuously in both time and space. For the unrelaxed case, Sandborn (11) recently suggested the start of the unrelaxed boundary layer separation could be taken as the forward most point where shear stress at the wall vanishes instantaneously.

Sandborn (11) further points out that the time required for the boundary layer to adjust to the changes at the boundaries appears to be the most important difference between the relaxed and unrelaxed separations.

There is increasing evidence that relaxation time for shear flow development at separation appears to be one of the important aspects of relaxed separation. Lighthill (5) analyzed the response of the laminar boundary layer to fluctuations in the oncoming stream, when the stream fluctuates in magnitude but not in direction. Stuart (19) derived an exact solution of the Navier-Stokes equations, where the

free stream velocity fluctuates about a constant mean, and velocity normal to the wall is constant. Both Lighthill's and Stuart's studies demonstrate that adjustment time is important in determining the velocity profile of a time varying shear flow. Sandborn (11) explored a pulsing flow, where a pulsing free stream velocity was produced by a siren, and found that the profile correlations at separation fall on the proposed empirical unrelaxed separation criterion. Sandborn's test thus constitutes an experimental proof of the new concept. But so far there appears to be no well defined parameters to specify limits for relaxed and unrelaxed separations.

The present analysis investigates a particular type of time varying shear flow, to study time adjustment effects on separation. A pipe flow that has a regular fluctuating velocity superimposed on the mean flow is analyzed. The velocity distributions and the velocity profile parameters, displacement thickness, momentum thickness, and form factor, are computed from a computer program. The results are compared with the model for relaxed and unrelaxed separation proposed by Sandborn and Kline. For high frequencies the boundary layer has little time to adjust, so the instantaneous zero wall shear stress profile correlations fall on the unrelaxed separation curve. For low frequencies there exists sufficient flow time for the boundary layer to adjust to the absence of a viscous force at the surface, thus the separation profile correlations agree with the relaxed separation curve. Stuart's solution is also analyzed. The results again agree with the proposed new concept, i.e., adjustment time is important in determining relaxed or unrelaxed separation. Separation criteria in terms of the non-dimensional pressure gradient parameter $(\frac{\theta^2}{\nu} \frac{1}{U} \frac{dU}{dt})$

and the velocity profile form factor are also given for both the unsteady pipe flow and Stuart's solution. The results show the separation velocity profiles may not be a one parameter family of velocity profiles as implied by the separation model of Sandborn (11).

Chapter II

REVIEW OF LITERATURE

2.1 Introduction

Sandborn (12) developed an empirical velocity profile that can be used in laminar as well as turbulent flow. From the analysis of this empirical velocity profile, two types of separation, relaxed (steady) and unrelaxed (unsteady), were identified. For the unrelaxed case the empirical relation among the profile parameters was given as

$$H = 1 + \frac{1}{(1 - \delta^*/\delta)} \quad (2-1)$$

For the relaxed separation case the relation between the profile parameters can be given parametrically in terms of λ_δ

$$\frac{\delta^*}{\delta} = \frac{2\sqrt{-\lambda_\delta} + 1}{(\sqrt{-\lambda_\delta} + 1)^2} \quad (2-2a)$$

$$\frac{\theta}{\delta} = \frac{(2\sqrt{-\lambda_\delta} + 1)}{(\sqrt{-\lambda_\delta} + 1)^2} - \frac{2(\sqrt{-\lambda_\delta})^2}{(2\sqrt{-\lambda_\delta} + 1)^3} - \frac{2\sqrt{-\lambda_\delta}}{(2\sqrt{-\lambda_\delta} + 1)^2} - \frac{1}{(2\sqrt{-\lambda_\delta} + 1)} \quad (2-2b)$$

where

$$\lambda_\delta = \frac{-\delta^2 dU}{\nu dx}$$

Equations 2-1 and 2-2 are replotted in Figure 1. The upper curve is called the relaxed, $\bar{\tau}_w = 0$, separation correlation, while the lower one corresponds to the unrelaxed separation correlation. Both the relaxed and unrelaxed separation curves shown on Figure 1 have been

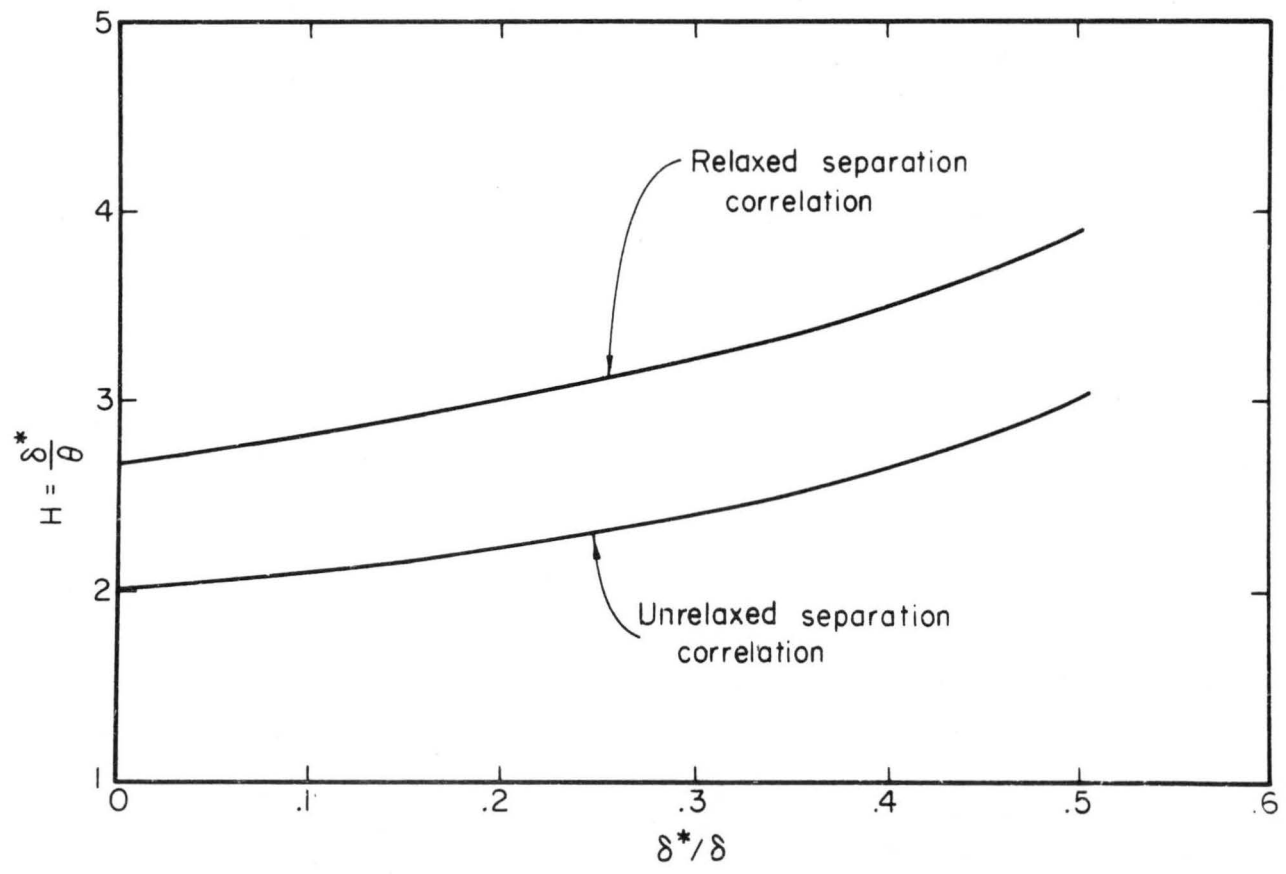


Figure 1 Relaxed and unrelaxed separation correlations

found, by Sandborn and Kline (13), to agree well with experimental measurements as well as with analytic solutions.

Many solutions of the laminar boundary layer equations for a steady two-dimensional incompressible flow have been evaluated analytically or numerically for various forms of free stream velocity distributions $U(x)$, for example, by Schlichting (15), Thwaites (20), Head and Hagasi (3), and Curle (1). The velocity components, u and v , as well as the variations with x of the skin friction and the momentum and displacement thickness, can be calculated to the separation point. For the solutions of unsteady laminar boundary layer equations references can be made to Rosenhead (10) and Schlichting (15).

2.2 Lighthill's Theory of the Response of Skin Friction to Fluctuations in the Stream Velocity

Lighthill (5) first treated the laminar boundary layer about a cylindrical body when the velocity of the oncoming flow oscillated in magnitude but not in direction. For high-frequency approximation, Lighthill obtained a solution identical to the solution for the shear-wave boundary layer, whose main stream fluctuates about a zero mean. Physically it means the effect of viscosity can be felt for the oscillation only within the small layer near the wall, with thickness of order $\sqrt{\nu/\omega}$. In other words, at high frequencies the fluctuating part of the velocity responds instantly, except within the very thin shear-wave boundary layer close to the wall. For low-frequency approximation, Lighthill used a Karman-Pohlhausen method (9) to solve the equations and found velocity fluctuation approximately consists of a part depending on the instantaneous stream velocity and a part depending on the stream acceleration.

Skin friction for both high-frequency and low-frequency approximations has a phase lead over the velocity fluctuation of the stream. The critical frequency separating the ranges of validity of the high- and low-frequency approximations is suggested by Lighthill as

$$\omega = \frac{3\tau_0}{\rho U_0 \delta_0^*} = \omega_0 \quad (2-3)$$

For frequencies $\omega < \omega_0$, both the amplitude and phase lead increase with frequency, the latter rises from zero to $\pi/4$; for frequencies $\omega > \omega_0$, the phase lead has the constant value $\pi/4$, and the amplitude increases with the square root of the frequency. The theory thus illustrates the large influence which a fluctuation has upon the transient velocity distributions and skin friction.

2.3 Fluctuating Flow Past an Infinite Flat Plate with Suction

Based on the classical exact "asymptotic suction" solution of steady flows developed by Schlichting (15), Stuart derived an exact solution of the Navier-Stokes equations, where the free stream velocity fluctuates about a constant mean and the normal velocity is constant toward the wall. It was found that for low frequencies the velocity distributions are closely approximated as the sum of parts proportional to the instantaneous velocity and acceleration of the main stream. For high frequencies the solution tends to the shear-wave solution with a periodic boundary layer without a mean flow as described by Lighthill.

Furthermore, the skin-friction fluctuations show much the same characteristics as that of Lighthill's. The amplitude of the skin-friction fluctuations rises with frequency, while the phase lead of

the skin-friction over the main stream velocity fluctuation rises from zero at zero frequency to $\pi/4$ at very high frequencies. The velocity profiles and skin-friction for Stuart's solution will be further analyzed in Chapter III. In particular, detailed evaluation of the boundary layer parameters and the velocity distributions at separation is made.

2.4 Unsteady Flow Through a Pipe

Several solutions for the flow through a long straight pipe under the influence of an unsteady pressure gradient have been reported. Sexl (16) first derived the solution for a pipe flow due to a periodic pressure gradient. Ito (4) considered the cases: (1) a pressure gradient changes linearly with time, (2) a pressure gradient that changes impulsively from one value to another, and (3) a damped oscillatory pressure gradient. The solutions were obtained by using a Laplace-transform technique.

For the case of the flow with a periodic pressure gradient the solution was given by Sexl as

$$u(r,t) = \frac{-ik}{\omega} e^{i\omega t} \left\{ 1 - \frac{J_0(r\sqrt{-i\omega/\nu})}{J_0(R\sqrt{-i\omega/\nu})} \right\} \quad (2-4)$$

where J_0 denotes the Bessel function of the first kind and of zeroth order.

The velocity distributions for both low- and high-frequency approximations were evaluated. For very low frequencies, the velocity distribution was found to be in phase with the pressure distribution,

the amplitude being a parabolic function of the radius, as was the case in steady flow. For very high frequencies, the phase shift of the flow at a large distance from the wall is $\pi/2$ with respect to the exciting force. No specific evaluation of $\tau_w = 0$ profiles has been made.

Chapter III

ANALYSIS OF UNSTEADY PIPE FLOW SEPARATION AND SEPARATION
IN FLUCTUATING FLOW PAST A POROUS FLAT PLATE3.1 Unsteady Pipe Flow

3.1.1 Solutions of unsteady pipe flow - The time varying pressure gradient flow in a pipe was solved independently of the studies discussed in Chapter II. Let x denote the coordinate in the direction of the axis of the pipe, r denote the radial distance from the axis, and u is the velocity component in x -direction. For a very long pipe, the velocity variations with x are negligible and the only component of the flow is u . Thus, the laminar boundary layer equation for the unsteady axially symmetrical pipe flow with constant density ρ and kinematic viscosity ν takes the form

$$\frac{\partial u}{\partial t} = -\frac{1}{\rho} \frac{\partial P}{\partial x} + \nu \frac{\partial^2 u}{\partial r^2} + \frac{\nu}{r} \frac{\partial u}{\partial r} \quad (3-1)$$

The boundary conditions are

$$u = 0 \quad \text{at} \quad r = R$$

and

$$u = U \quad \text{at} \quad r = 0 \quad .$$

(3-2)

We assume that the pressure gradient fluctuates about a constant mean and is given by

$$-\frac{1}{\rho} \frac{\partial P}{\partial x} = K(1 + \epsilon e^{i\omega t}) \quad (3-3)$$

where K is a constant, and $K\epsilon$ is the amplitude of fluctuations.

Now we are seeking a solution of the form

$$u = U_0 [\zeta_0(r) + \epsilon \zeta_1(r) e^{i\omega t}] \quad (3-4)$$

in which U_0 is the mean velocity along the axis as obtained for Poiseuille flow. Substituting Equations 3-3 and 3-4 in Equation 3-1 and equating non-periodic and periodic terms separately to zero, we have

$$r\zeta_0''(r) + \zeta_0'(r) = -\frac{rK}{\nu U_0} \quad (3-5)$$

$$\zeta_1''(r) + \frac{1}{r} \zeta_1'(r) - \frac{i\omega}{\nu} \zeta_1(r) = \frac{-K}{\nu U_0} . \quad (3-6)$$

Equation 3-5 is a second order nonhomogeneous differential equation, whereas Equation 3-6 is a Bessel equation of order zero with an imaginary parameter (21). The boundary conditions for Equation 3-5 are

$$\zeta_0'(r) = 0 \quad \text{at } r = 0 \quad , \quad \zeta_0(r) = 0 \quad \text{at } r = R \quad ,$$

$$\text{and } \zeta_0(r) = 1 \quad \text{at } r = 0 \quad , \quad (3-7)$$

and, hence, the solution is

$$\zeta_0(r) = \left(1 - \frac{r^2}{R^2}\right) \quad (3-8)$$

where use was made of the following relation

$$U_0 = KR^2/4\nu .$$

The boundary conditions for Equation 3-6 are

$$\zeta_1 = \text{finite at } r = 0 \quad , \quad \zeta_1 = 0 \quad \text{at } r = R \quad . \quad (3-9)$$

Expressing the solution of Equation 3-6 in terms of ber and bei functions, we obtained

$$\zeta_1(r) = \frac{\nu}{i\omega} \frac{4}{R^2} \left[1 - \frac{\text{ber} \sqrt{\frac{\omega}{\nu}} r + \text{bei} \sqrt{\frac{\omega}{\nu}} r}{\text{ber} \sqrt{\frac{\omega}{\nu}} R + \text{bei} \sqrt{\frac{\omega}{\nu}} R} \right] . \quad (3-10)$$

The total velocity component in x-direction becomes

$$u = U_0 \left[\left(1 - \frac{r^2}{R^2}\right) + \varepsilon e^{i\omega t} \frac{\nu}{i\omega} \frac{4}{R^2} \left(1 - \frac{\text{ber} \sqrt{\frac{\omega}{\nu}} r + \text{bei} \sqrt{\frac{\omega}{\nu}} r}{\text{ber} \sqrt{\frac{\omega}{\nu}} R + \text{bei} \sqrt{\frac{\omega}{\nu}} R} \right) \right] . \quad (3-11a)$$

The fluctuating part of Equation 3-11a is equivalent to Equation 2-4 obtained by Sexl (16). The transient velocity in the center reduces to

$$U = U_0 \left[1 + \epsilon e^{i\omega t} \frac{v}{i\omega} \frac{4}{R^2} \left(1 - \frac{1}{\text{ber} \sqrt{\frac{\omega}{v}} R + i \text{bei} \sqrt{\frac{\omega}{v}} R} \right) \right] . \quad (3-11b)$$

The shear stress at the wall is

$$\begin{aligned} \tau_w &= \mu \left. \frac{\partial u}{\partial r} \right|_{r=R} \\ &= -\mu U_0 \frac{2}{R} \left[1 + \epsilon e^{i\omega t} \frac{2}{iR} \sqrt{\frac{\omega}{v}} \frac{\text{ber}' \sqrt{\frac{\omega}{v}} R + i \text{bei}' \sqrt{\frac{\omega}{v}} R}{\text{ber} \sqrt{\frac{\omega}{v}} R + i \text{bei} \sqrt{\frac{\omega}{v}} R} \right] \end{aligned} \quad (3-12)$$

where primes denote differentiation with respect to r , and

$$\text{ber } x = \sum_{j=0}^{\infty} \frac{(-1)^j x^{4j}}{2^{4j} [(2j)!]^2}$$

$$\text{bei } x = \sum_{j=0}^{\infty} \frac{(-1)^j x^{4j+2}}{2^{4j+2} [(2j+1)!]^2}$$

$$\text{ber}' x = \sum_{j=1}^{\infty} \frac{(-1)^j 4j x^{4j-1}}{2^{4j} [(2j)!]^2}$$

$$\text{bei}' x = \sum_{j=0}^{\infty} \frac{(-1)^j (4j+2) x^{4j+1}}{2^{4j+2} [(2j+1)!]^2}$$

Plots of $\text{ber } x$, $\text{bei } x$, $\text{ber}' x$, and $\text{bei}' x$ are shown in Figure 2.

The graphs are seen to oscillate with ever-increasing amplitudes.

Table 1 shows the variations with x of $\text{ber } x$, $\text{bei } x$, $\text{ber}' x$, and $\text{bei}' x$ from $x = 0$ to $x = 80$.

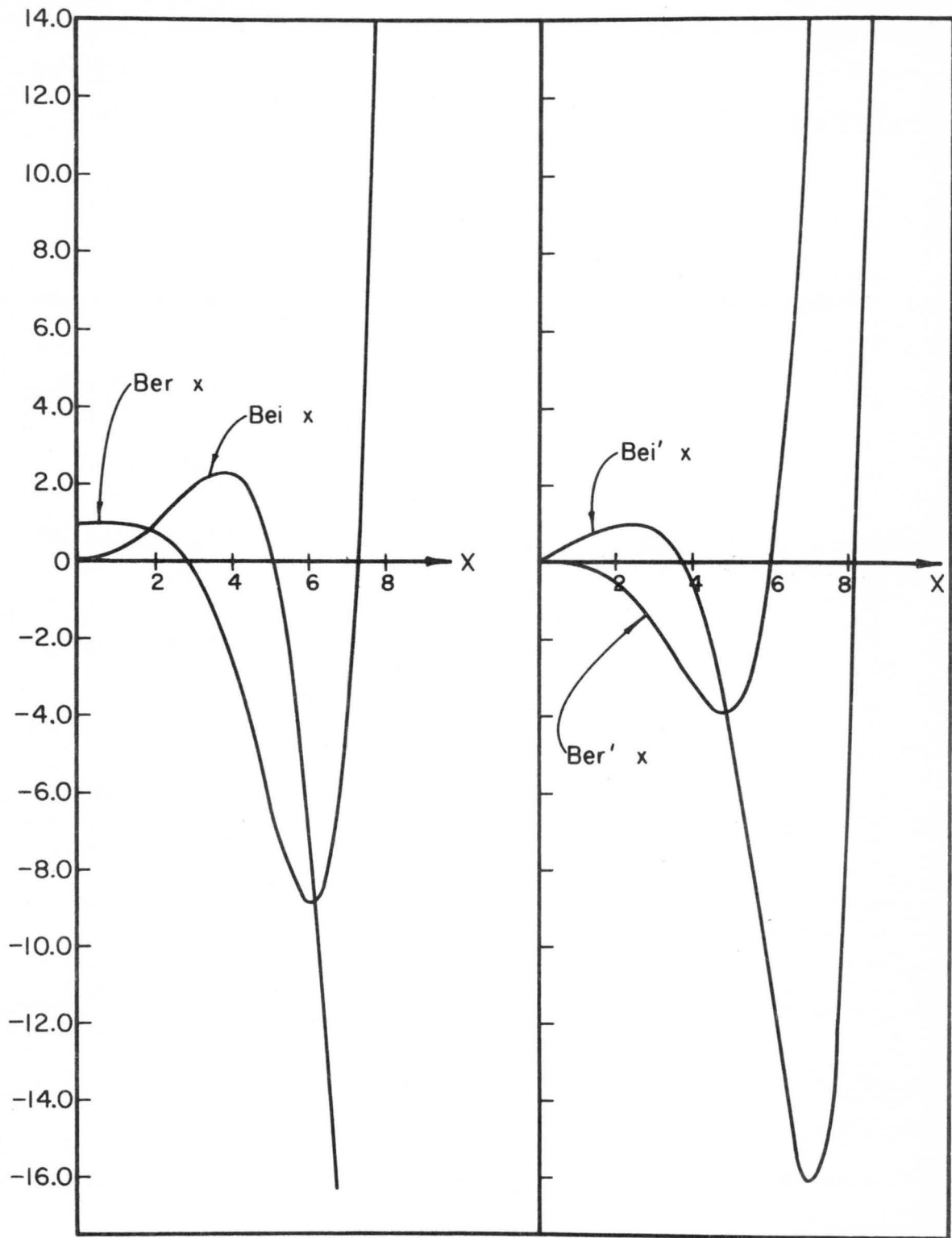


Figure 2 Plots showing the functions $Ber\ x$, $Bei\ x$, $Ber'\ x$, and $Bei'\ x$

3.1.2 Velocity distributions and velocity profile parameters at separation - The real parts of Equation 3-11 and Equation 3-12 reduce to

$$\frac{u}{U_0} = 1 - \left(\frac{r}{R}\right)^2 + \epsilon \frac{4}{\frac{\omega}{\nu} R^2} \left[\cos \omega t \frac{(\text{bei} \sqrt{\frac{\omega}{\nu}} R) (\text{ber} \sqrt{\frac{\omega}{\nu}} r) - (\text{ber} \sqrt{\frac{\omega}{\nu}} R) (\text{bei} \sqrt{\frac{\omega}{\nu}} r)}{(\text{ber} \sqrt{\frac{\omega}{\nu}} R)^2 + (\text{bei} \sqrt{\frac{\omega}{\nu}} R)^2} \right. \\ \left. + \sin \omega t - \sin \omega t \frac{(\text{ber} \sqrt{\frac{\omega}{\nu}} R) (\text{ber} \sqrt{\frac{\omega}{\nu}} r) + (\text{bei} \sqrt{\frac{\omega}{\nu}} R) (\text{bei} \sqrt{\frac{\omega}{\nu}} r)}{(\text{ber} \sqrt{\frac{\omega}{\nu}} R)^2 + (\text{bei} \sqrt{\frac{\omega}{\nu}} R)^2} \right] \quad (3-13a)$$

$$\frac{U}{U_0} = 1 + \epsilon \frac{4}{\frac{\omega}{\nu} R^2} \left[\frac{\text{bei} \sqrt{\frac{\omega}{\nu}} R}{(\text{ber} \sqrt{\frac{\omega}{\nu}} R)^2 + (\text{bei} \sqrt{\frac{\omega}{\nu}} R)^2} \cos \omega t \right. \\ \left. + \sin \omega t - \frac{\text{ber} \sqrt{\frac{\omega}{\nu}} R}{(\text{ber} \sqrt{\frac{\omega}{\nu}} R)^2 + (\text{bei} \sqrt{\frac{\omega}{\nu}} R)^2} \sin \omega t \right] \quad (3-13b)$$

$$\tau_w = -\mu U_0 \frac{2}{R} \left[1 + \frac{2}{R} \sqrt{\frac{\nu}{\omega}} \epsilon \left\{ \cos \omega t \frac{(\text{ber} \sqrt{\frac{\omega}{\nu}} R) (\text{bei}' \sqrt{\frac{\omega}{\nu}} R) - (\text{bei} \sqrt{\frac{\omega}{\nu}} R) (\text{ber}' \sqrt{\frac{\omega}{\nu}} R)}{(\text{ber} \sqrt{\frac{\omega}{\nu}} R)^2 + (\text{bei} \sqrt{\frac{\omega}{\nu}} R)^2} \right. \right. \\ \left. \left. + \sin \omega t \frac{(\text{ber} \sqrt{\frac{\omega}{\nu}} R) (\text{ber}' \sqrt{\frac{\omega}{\nu}} R) + (\text{bei} \sqrt{\frac{\omega}{\nu}} R) (\text{bei}' \sqrt{\frac{\omega}{\nu}} R)}{(\text{ber} \sqrt{\frac{\omega}{\nu}} R)^2 + (\text{bei} \sqrt{\frac{\omega}{\nu}} R)^2} \right\} \right] \quad (3-14)$$

respectively.

The shear stress, τ_w , is zero when the coefficient of ϵ in Equation 3-14 is equal to $-1/\epsilon$ which corresponds to a velocity profile with zero skin friction. Thus the velocity profiles at separation can be obtained by substituting

$$\begin{aligned}
-\frac{1}{\varepsilon} = & \left[\cos \omega t \frac{(\text{ber} \sqrt{\frac{\omega}{\nu}} R)(\text{bei}' \sqrt{\frac{\omega}{\nu}} R) - (\text{bei} \sqrt{\frac{\omega}{\nu}} R)(\text{ber}' \sqrt{\frac{\omega}{\nu}} R)}{(\text{ber} \sqrt{\frac{\omega}{\nu}} R)^2 + (\text{bei} \sqrt{\frac{\omega}{\nu}} R)^2} \right. \\
& \left. + \sin \omega t \frac{(\text{ber} \sqrt{\frac{\omega}{\nu}} R)(\text{ber}' \sqrt{\frac{\omega}{\nu}} R) + (\text{bei} \sqrt{\frac{\omega}{\nu}} R)(\text{bei}' \sqrt{\frac{\omega}{\nu}} R)}{(\text{ber} \sqrt{\frac{\omega}{\nu}} R)^2 + (\text{bei} \sqrt{\frac{\omega}{\nu}} R)^2} \right] \frac{2}{R} \sqrt{\frac{\nu}{\omega}}
\end{aligned}
\tag{3-15}$$

in Equation 3-13.

Figure 3 shows the velocity profiles at separation for various frequencies, where y is the vertical distance from the wall. Figure 4 compares the high frequency separation velocity profile with the velocity profile for steady flow, and the low frequency separation velocity profile with the relaxed separation velocity profile of Equation 2-2. For high frequencies (large values of $\sqrt{\frac{\omega}{\nu}} R$), viscosity does not have time to adjust the velocity to the changes imposed by the exciting pressure-gradient fluctuations, except in a 'shear-wave layer' near the wall. The high frequency separation profile remains the same as the velocity profile for steady flow, except in a thin layer near the wall where the effect of viscosity can be felt for the oscillations. Thus the high frequency separation belongs to the class of unrelaxed separation profiles as will be demonstrated later. On the other hand, for very low frequencies the solution corresponds to the quasi-steady solution. The separation profile has a good agreement with the relaxed separation profile of Equation 2-2, with the same form factor, H . This comparison supports the evidence that adjustment time is an important factor for separation to be relaxed or unrelaxed, the concept proposed by Sandborn (11).

It has been found that some separation velocity profiles of Equation 3-13 can only occur in unsteady flow. These profiles are not

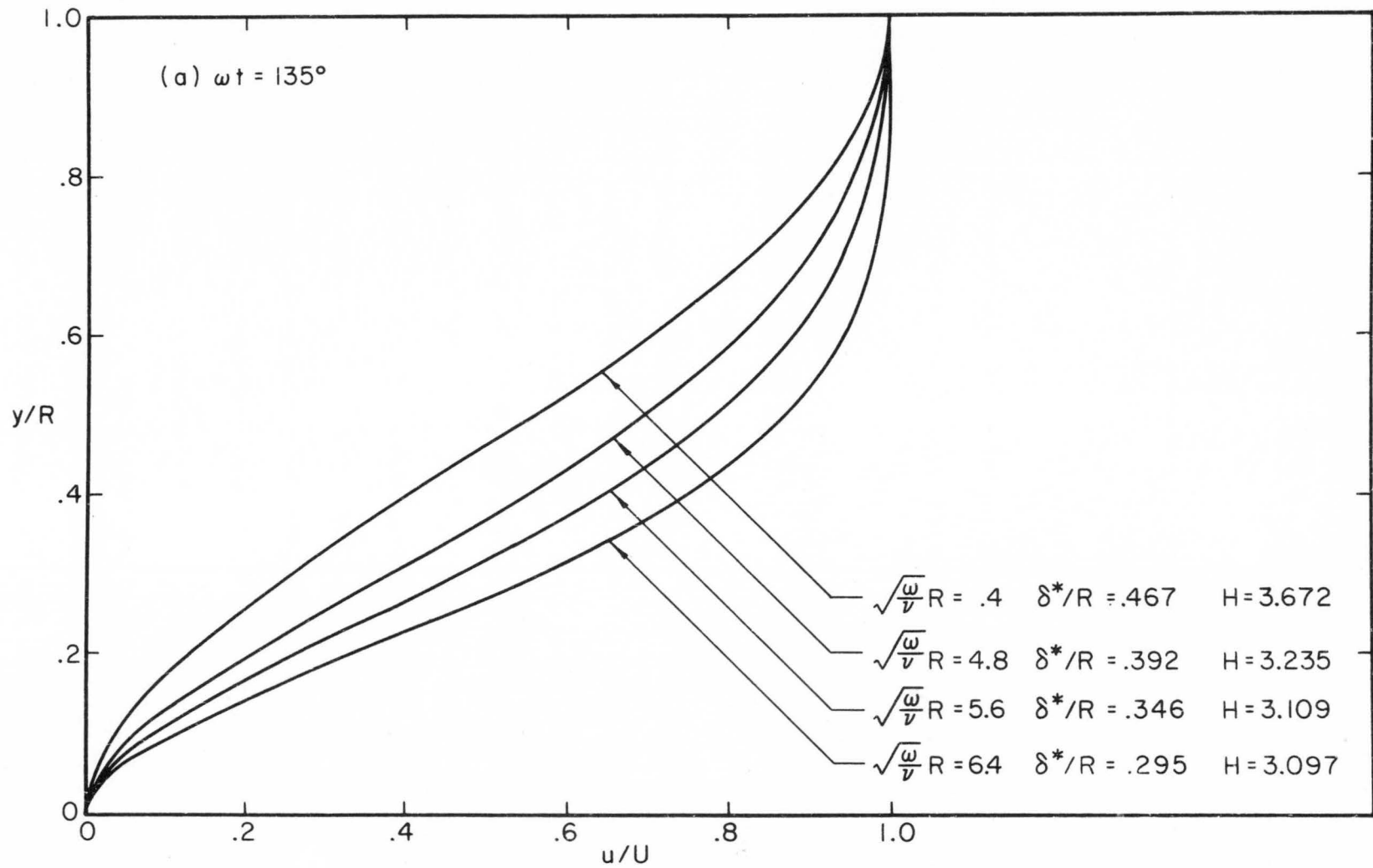


Figure 3 Velocity profiles at separation for time varying pipe flow

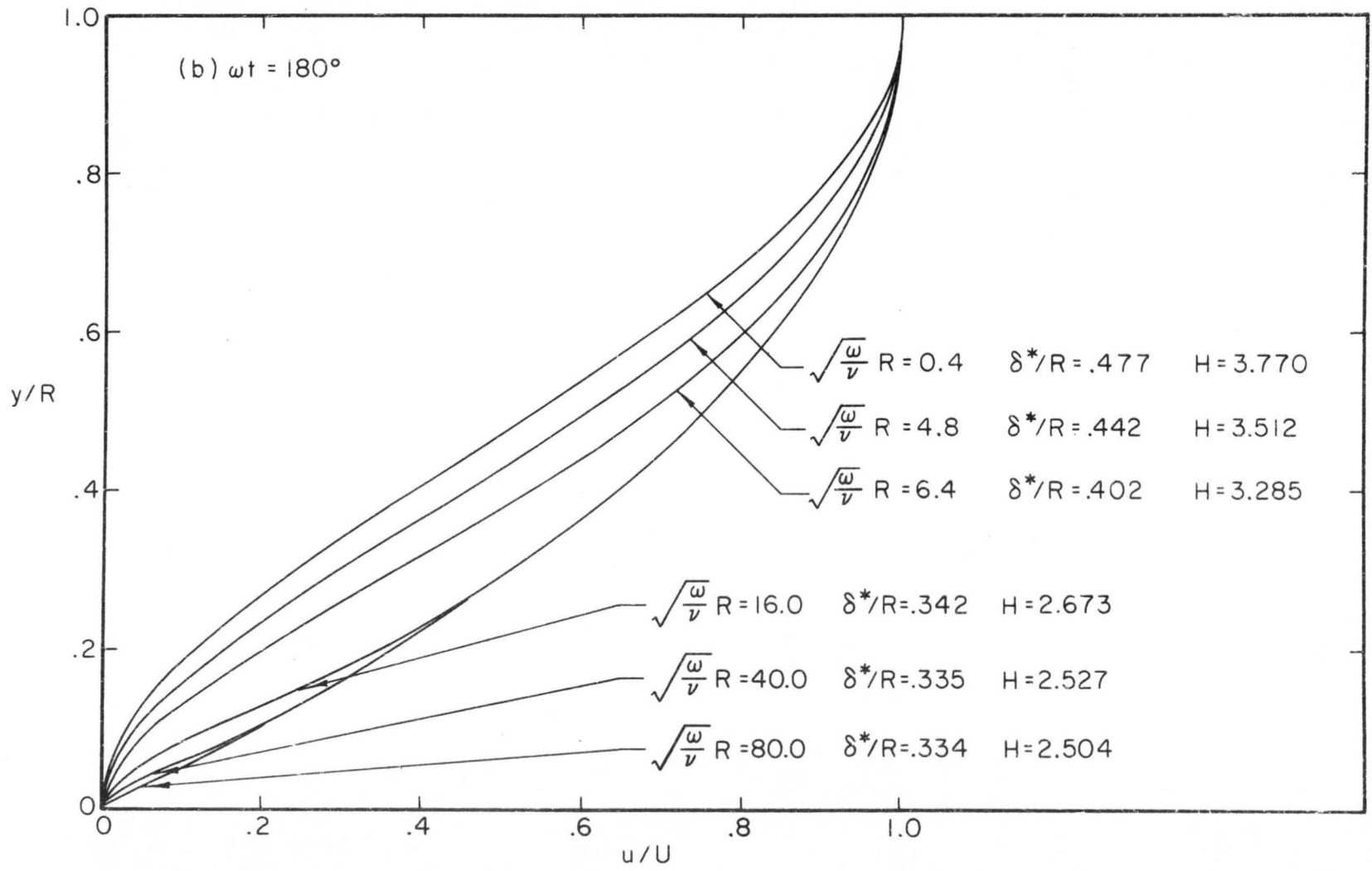


Figure 3 Continued

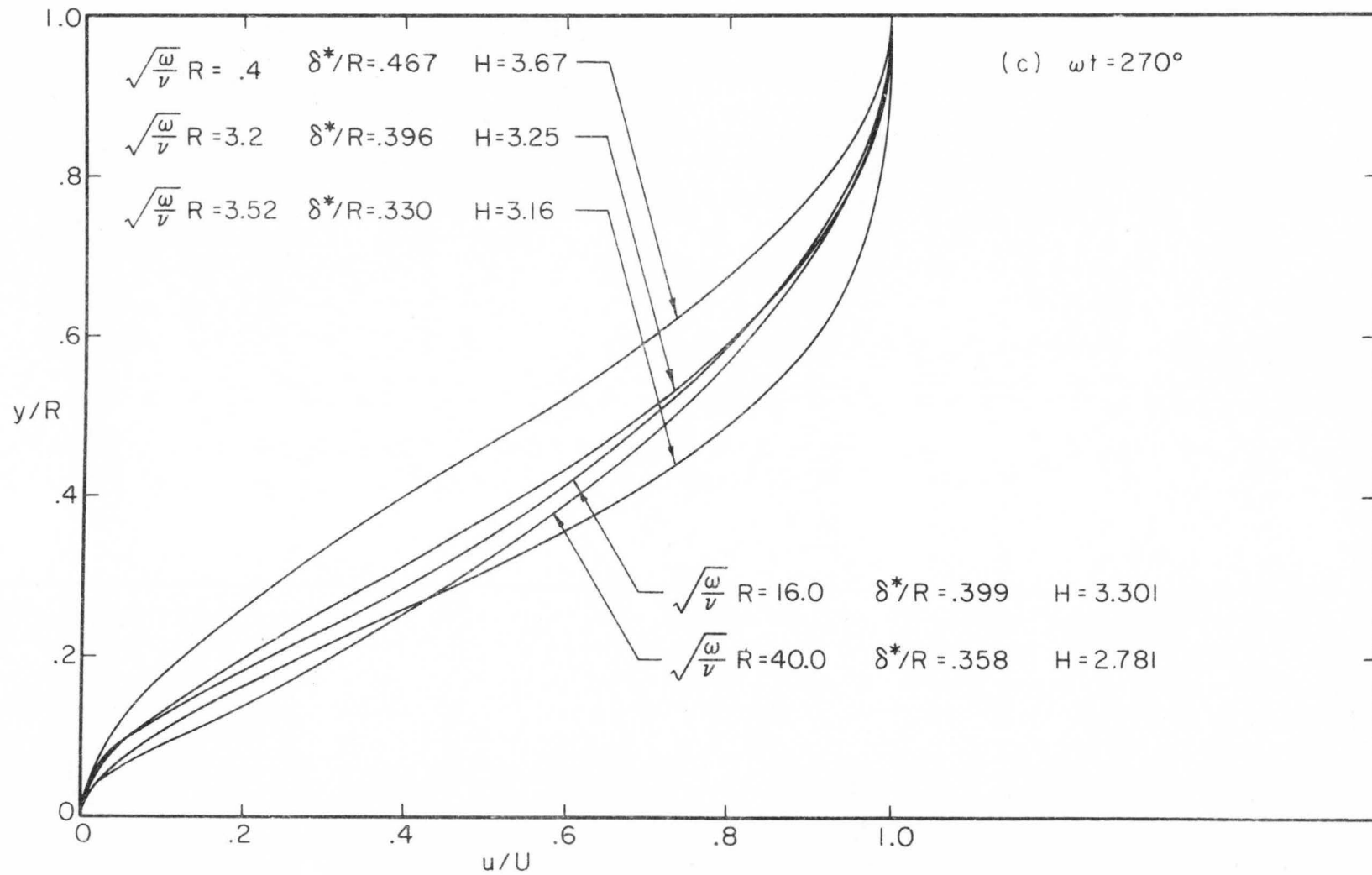


Figure 3 Continued

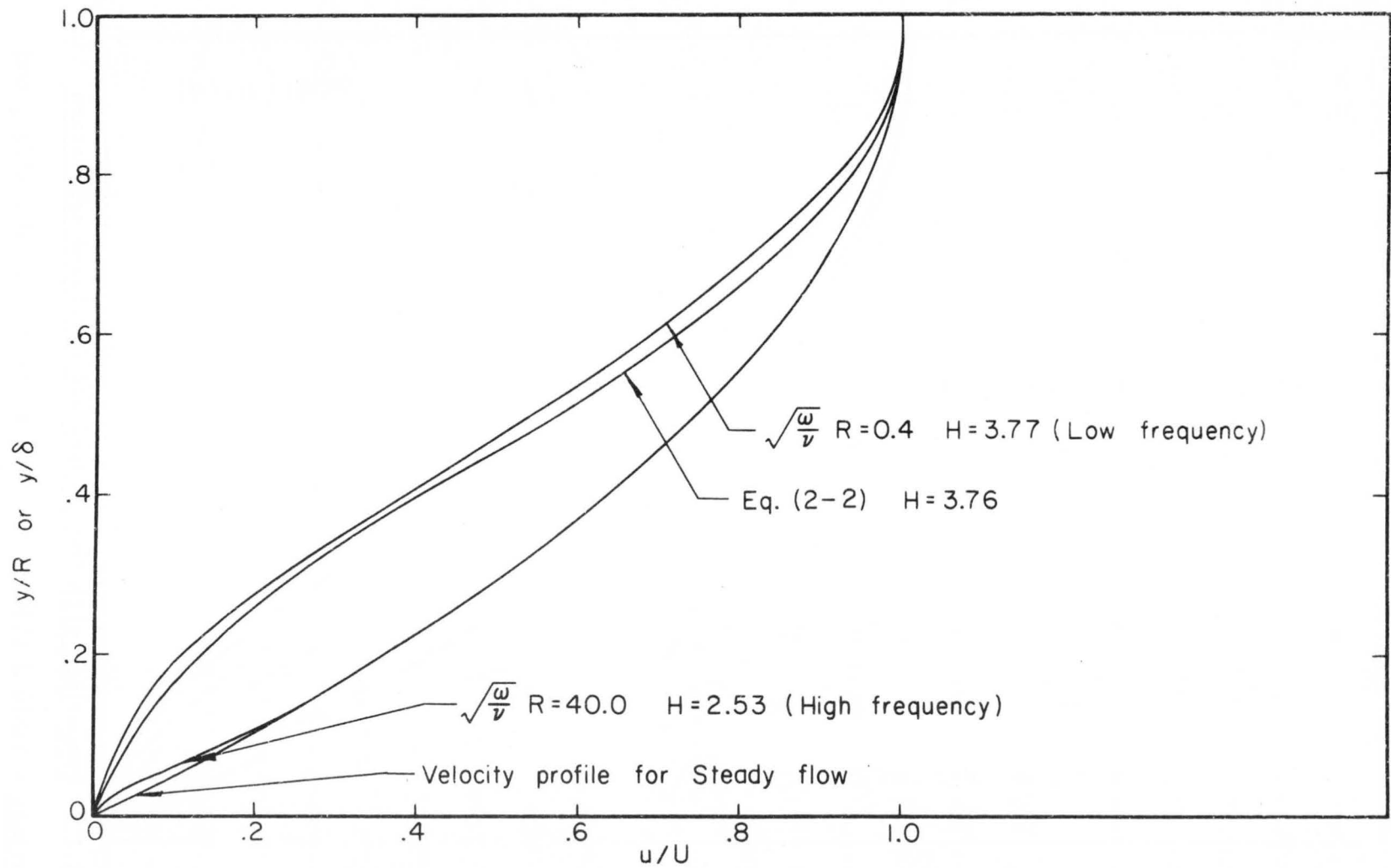


Figure 4 Comparison of the high frequency separation profile with the velocity profile for steady flow, and the low frequency separation profile with the relaxed separation profile of Eq. (2-2).

likely to occur in a boundary layer type flow. Figure 5 gives examples of such separation profiles including: (1) a velocity profile which is not monotonic, (2) values $u/U > 1$ occur in the velocity profile, and (3) a velocity profile with reverse flow.

The variations of ϵ with respect to $\sqrt{\frac{\omega}{\nu}} R$ for several values of ωt , as calculated from Equation 3-15, are plotted in Figure 6. For high frequencies, the values of ϵ for which separation occurs, are large. When frequencies decrease, separation is reached in most cases for smaller values of ϵ . This result is different from the results obtained by Stuart.

The velocity profile parameters, displacement thickness δ^* , momentum thickness θ , and form factor H , are defined as:

$$\delta^* = \int_{y=0}^{\infty} \left(1 - \frac{u}{U}\right) dy, \quad \theta = \int_{y=0}^{\infty} \frac{u}{U} \left(1 - \frac{u}{U}\right) dy, \quad H = \frac{\delta^*}{\theta} \quad (3-16)$$

respectively.

Profile parameters at separation for various frequencies and ωt 's are computed from a computer program. In calculating these parameters 40 mesh points were taken across each velocity profile. The relationship between the form factor H and ratio of δ^*/δ is compared with the relaxed and unrelaxed separation correlation criteria, proposed by Sandborn and Kline (13), in Section 3.1.3. It is well known that the laws of flow deduced from the study of flows through pipe can be applied to the description of the flow in a boundary layer.

3.1.3 Comparison with the relaxed and unrelaxed separation correlations - Table 2 illustrates the variations of H , δ^*/δ , and

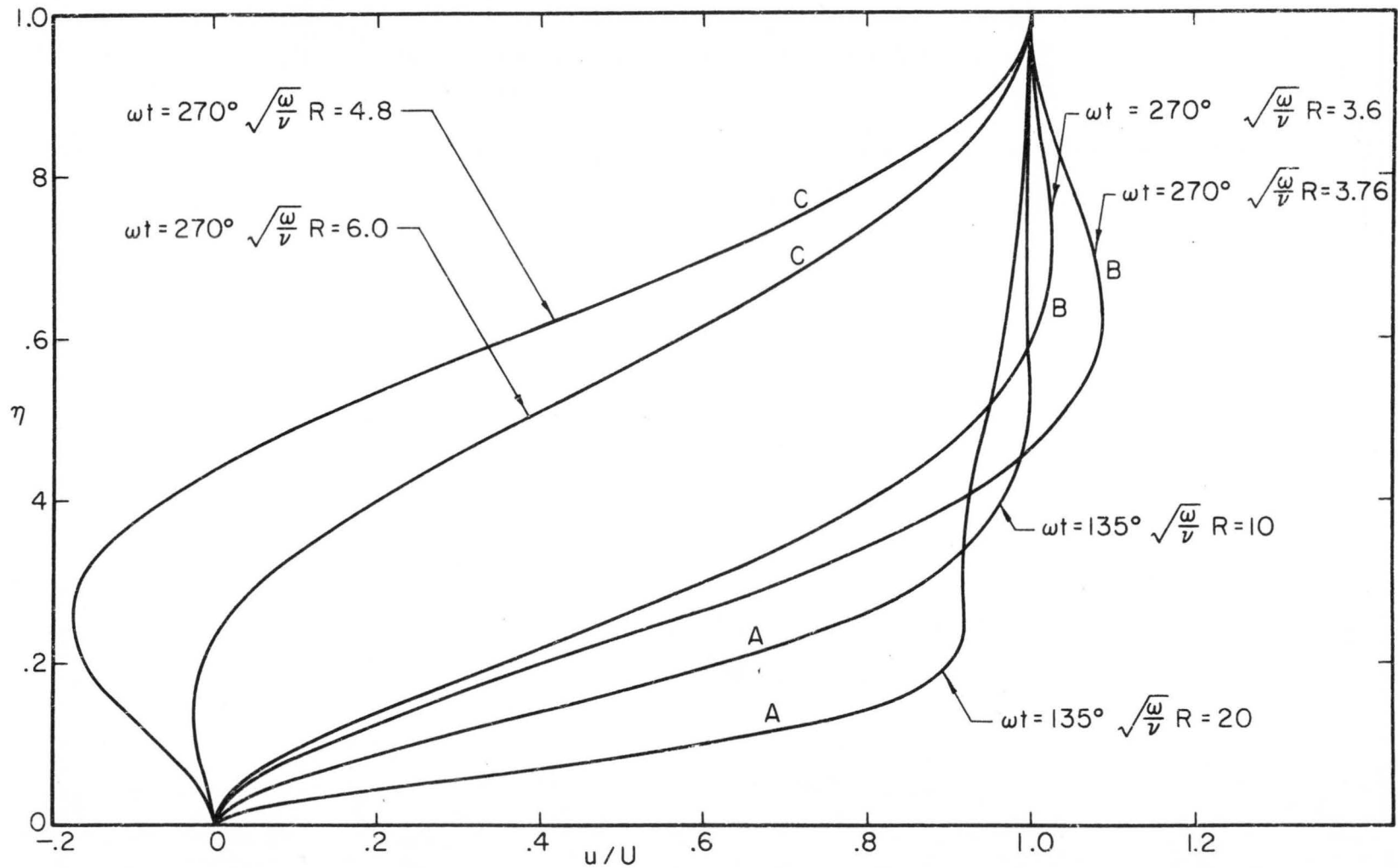


Figure 5 Some particular types of separation profiles in time varying pipe flow calculated from Eq.(3-13) (A), a velocity profile which is not monotonic; (B) values u/U occur in the velocity profile; (C) a velocity profile with reverse flow.

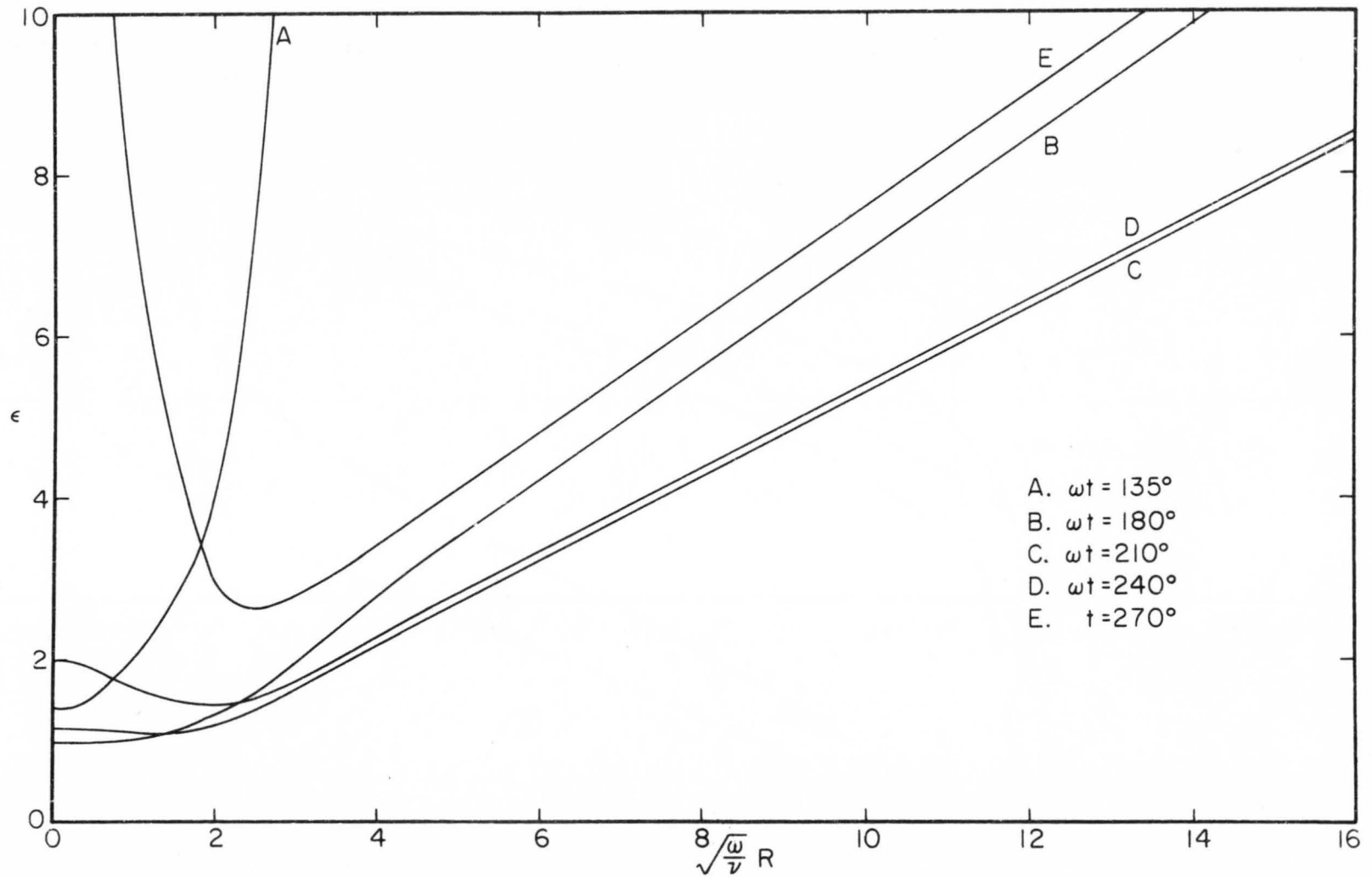


Figure 6 Variations of ϵ with respect to $\sqrt{\frac{\omega}{\nu}} R$ for time varying pipe flow at separation.

ϵ with respect to $\sqrt{\frac{\omega}{\nu}} R$ for various values of ωt . Figure 7 is a comparison of the separation profile parameters as calculated from Equations 3-13, 3-15, and 3-16, with the empirical relaxed and unrelaxed separation correlations. In plotting Figure 7, the separation profiles that have the same characteristics as described in Figure 5 are excluded. For very low frequencies, the separation correlations for all values of ωt fall almost on a simple curve, which is slightly below the empirical relaxed separation curve. As frequencies increase and reach a specific point where the value of δ^*/δ approximately equals 0.395, the correlation curves separate as illustrated in Figure 7. The values of $\sqrt{\frac{\omega}{\nu}} R$ where departure starts to occur are different for different values of ωt . For very high frequencies all the correlation curves appear to end at the same point directly on the empirical unrelaxed separation curve. The velocity profiles for very high and very low frequencies, as shown in Figure 4, agree well with the relaxed separation profile and the velocity profile for steady flow, respectively. This result suggests the empirical curves may be a reasonable approximation and confirms that adjustment time is an important factor in determining if separation is relaxed or unrelaxed. In Figure 7, it can also be seen that the transitions from the unrelaxed separation correlation to the relaxed separation correlation may be quite different. In determining if reverse flow occurs near the wall, 80 mesh points have been taken across the velocity profiles. The results are slightly different from that of only 40 mesh points. Therefore, in Figure 7 the points where the correlation curves are cut off are only approximate.

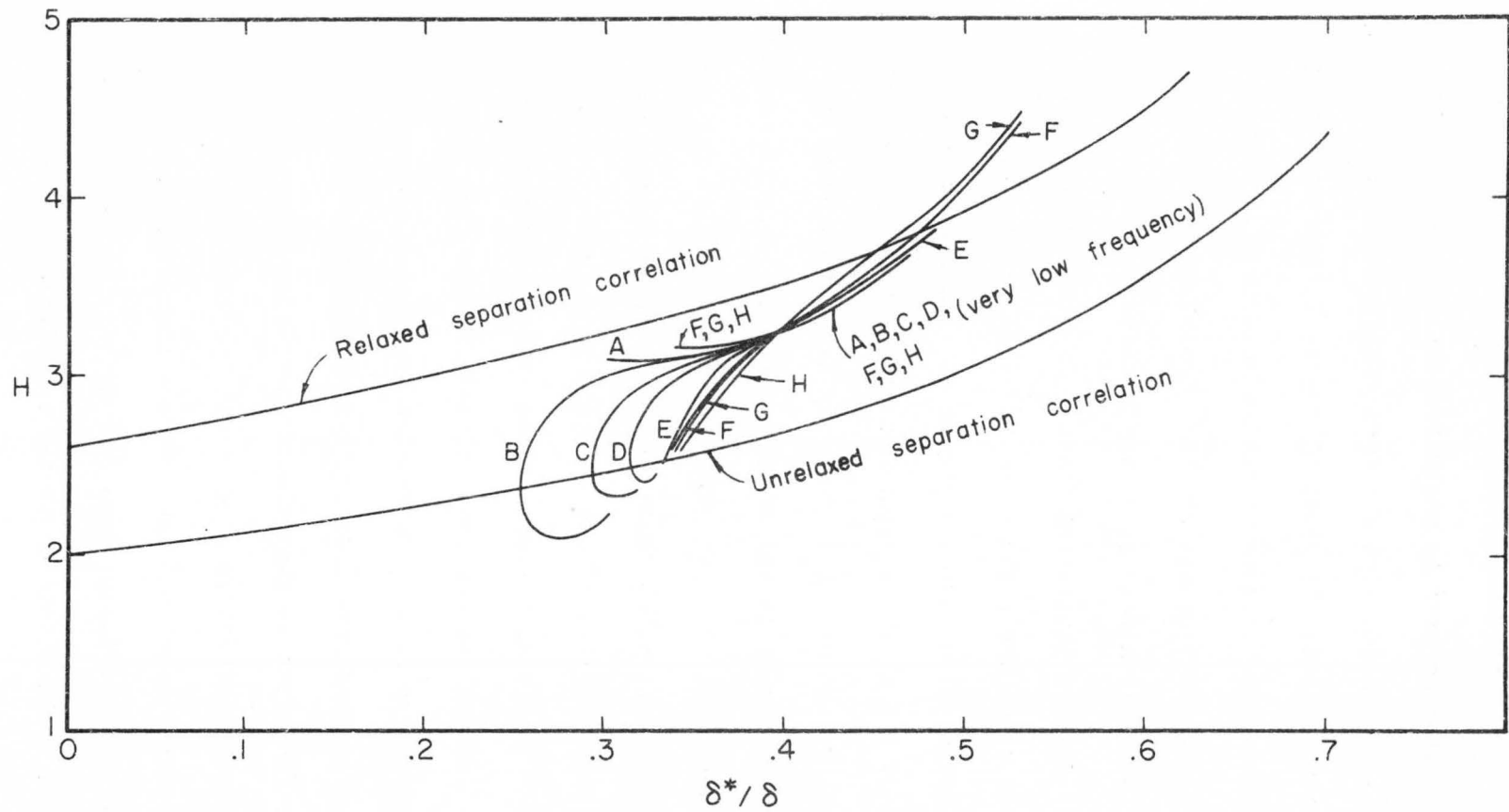


Figure 7 Comparison of time varying pipe flow separation profile parameters with the empirical relaxed and unrelaxed separation correlations for various ωt 's ; A, $\omega t = 135^\circ$; B, $\omega t = 142.5^\circ$; C, $\omega t = 150^\circ$; D, $\omega t = 157.5^\circ$; E, $\omega t = 180^\circ$; F, $\omega t = 210^\circ$; G, $\omega t = 240^\circ$; H, $\omega t = 270^\circ$.

As pointed out by Sandborn (11), these correlations of Figure 7 are not applicable in predicting separation, since it is nearly impossible to evaluate all of the three required parameters. In Figure 8 the form factor H is plotted against the pressure gradient parameter

$$\lambda_t = - \frac{R^2}{\nu} \frac{1}{U} \frac{dU}{dt} ,$$

which is similar to the parameter

$$\lambda_\delta = - \frac{\delta^2}{\nu} \frac{dU}{dx}$$

in the steady state flow. It can be seen that the three correlation curves for $\omega t = \pi$, $7/6\pi$, and $4/3\pi$ are consistent only when the parameter λ_t is greater than about 40. As shown in Figure 9, similar results are obtained when the form factor H is plotted against the pressure gradient parameter

$$\lambda_\theta = - \frac{\theta^2}{\nu} \frac{1}{U} \frac{dU}{dt} .$$

These results show velocity profiles at separation may not be a one parameter family of velocity profiles as implied by the separation model of Sandborn (11). It is suspected that this discrepancy may indicate the dependency on the time history is not adequately expressed by the classical pressure gradient parameter.

3.2 Fluctuating Flow Past a Porous Flat Plate

3.2.1 Velocity distributions and velocity profile parameters at separation - Stuart's solution for fluctuating flow past a flat plate with suction was reviewed in Chapter II. From Stuart's derivation we have

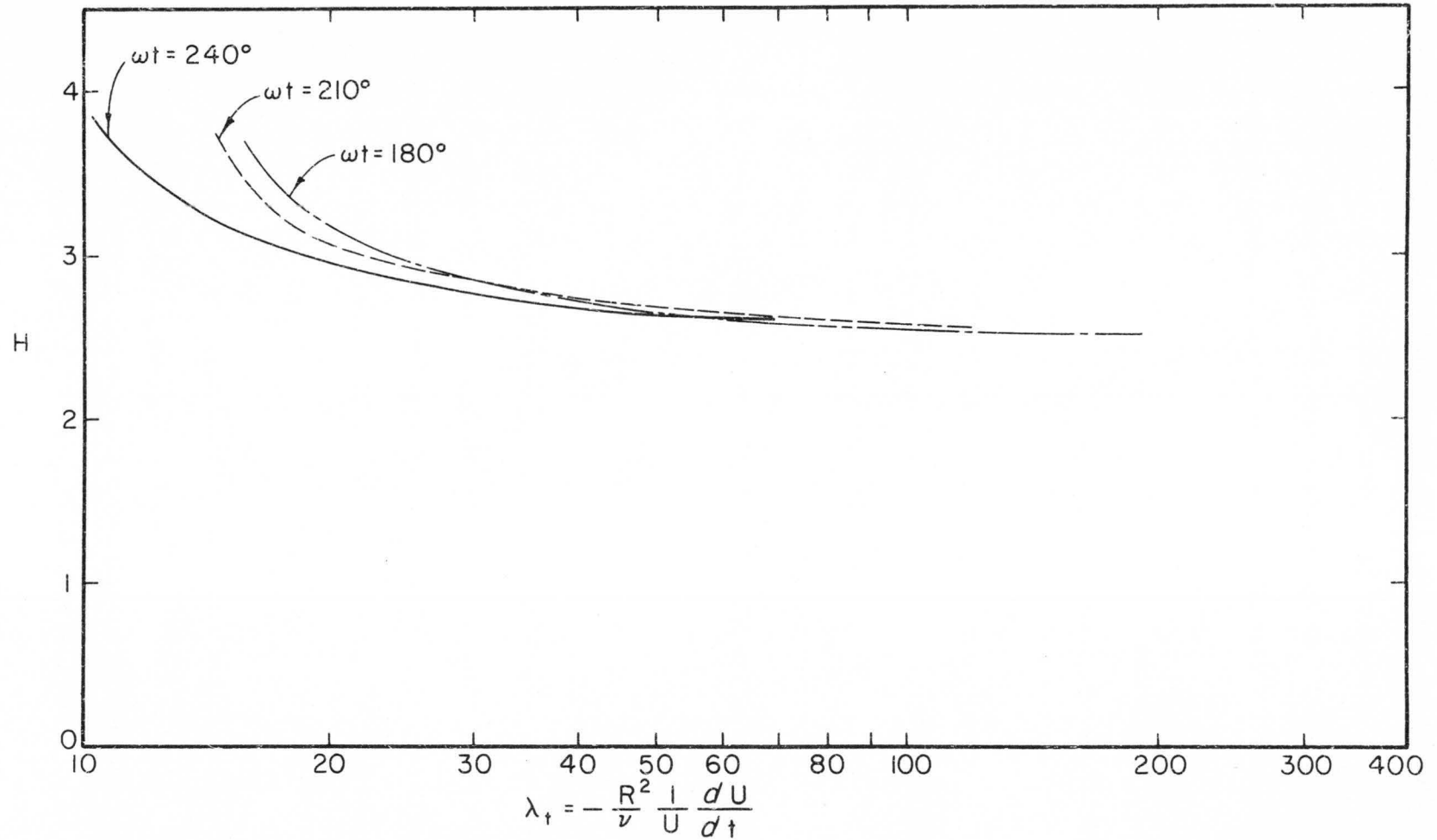


Figure 8 Variations of the form factor at separation with the pressure gradient parameter

$-\frac{R^2}{\nu} \frac{1}{U} \frac{dU}{dt}$ for time varying pipe flow.

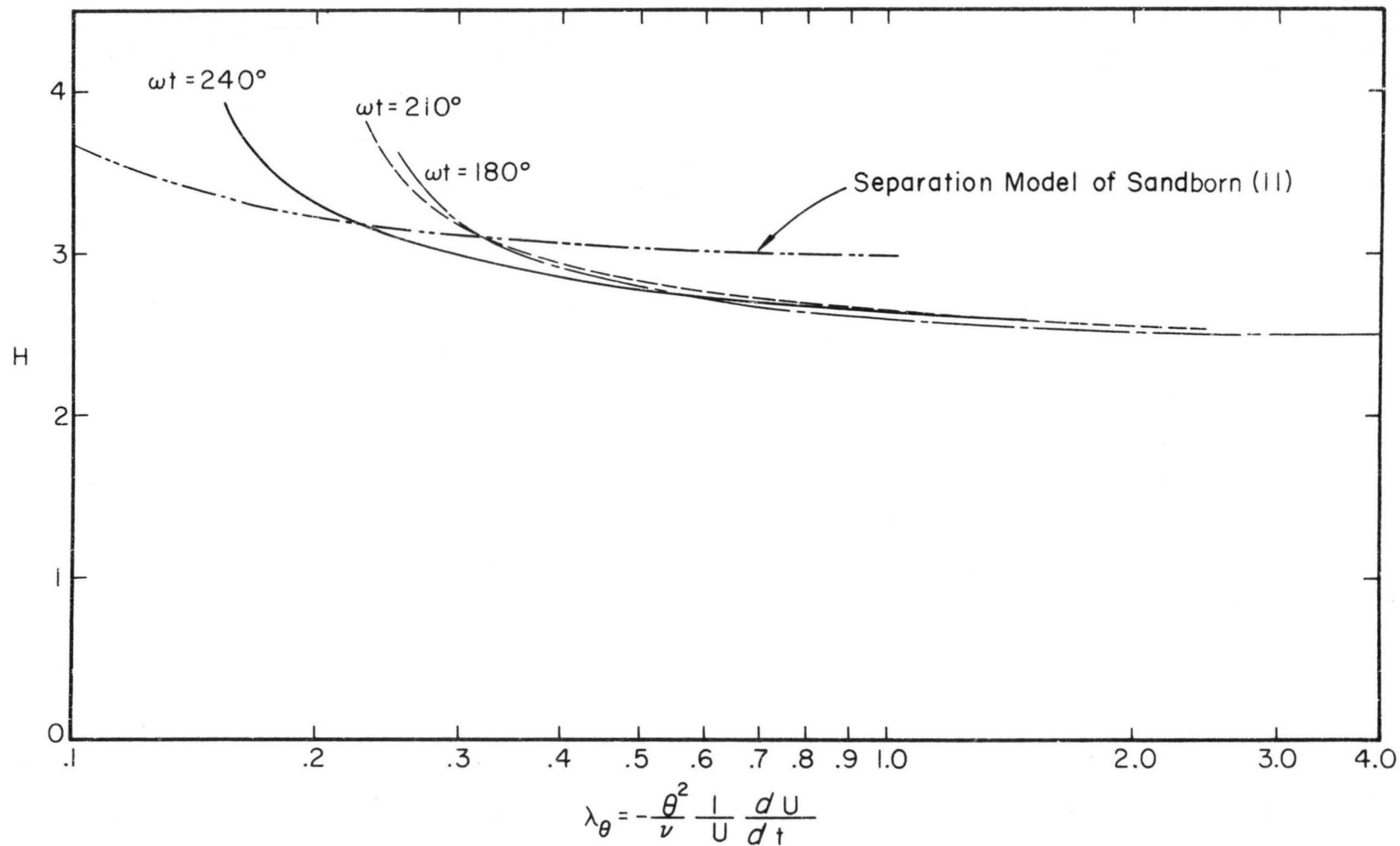


Figure 9 Variations of the form factor at separation with the pressure gradient parameter $-\frac{\theta^2}{\nu} \frac{1}{U} \frac{dU}{dt}$ for time varying pipe flow.

$$\frac{u}{U_0} = 1 - e^{-\eta} + \varepsilon \cos \omega t - \varepsilon e^{-h_r \eta} \cos(\omega t - h_i \eta) \quad (3-17a)$$

$$\frac{u}{U} = \left[1 - e^{-\eta} + \varepsilon \cos \omega t - \varepsilon e^{-h_r \eta} \cos(\omega t - h_i \eta) \right] \frac{1}{1 + \varepsilon \cos \omega t} \quad (3-17b)$$

The shear stress at the wall reduces to

$$\frac{\tau_w}{\rho U_0 |v_w|} = 1 + \varepsilon |h| \cos(\omega t + \alpha) \quad (3-18)$$

where

$$h = h_r + ih_i = \frac{1}{2} + \frac{1}{2} [1 + (4\lambda)^2]^{\frac{1}{4}} \cos\left(\frac{1}{2} \tan^{-1} 4\lambda\right) \\ + \frac{i}{2} [1 + (4\lambda)^2]^{\frac{1}{4}} \sin\left(\frac{1}{2} \tan^{-1} 4\lambda\right)$$

$$\alpha = \tan^{-1} h_i/h_r, \quad \lambda = \omega v/v_w^2$$

Provided $\varepsilon |h| \geq 1$, the shear stress, τ_w , is zero when

$$\cos(\omega t + \alpha) = -\frac{1}{\varepsilon |h|}, \quad (3-19)$$

which corresponds to a transient separation velocity profile. Figure 10 shows variations of ε and U/U_0 at separation with respect to λ for different values of ωt ; for high frequencies separation occurs at very small values of ε . The separation velocity profiles are plotted in Figure 11. From Figure 11 we can see that the high-frequency separation profiles become identical with the velocity profile for steady flow except in the layer near the wall where the separation profiles adjust to satisfy $\partial u/\partial y = 0$ at the wall. From Equations 3-17 and 3-19 the separation profile parameters, displacement thickness and momentum thickness, are obtained in the form

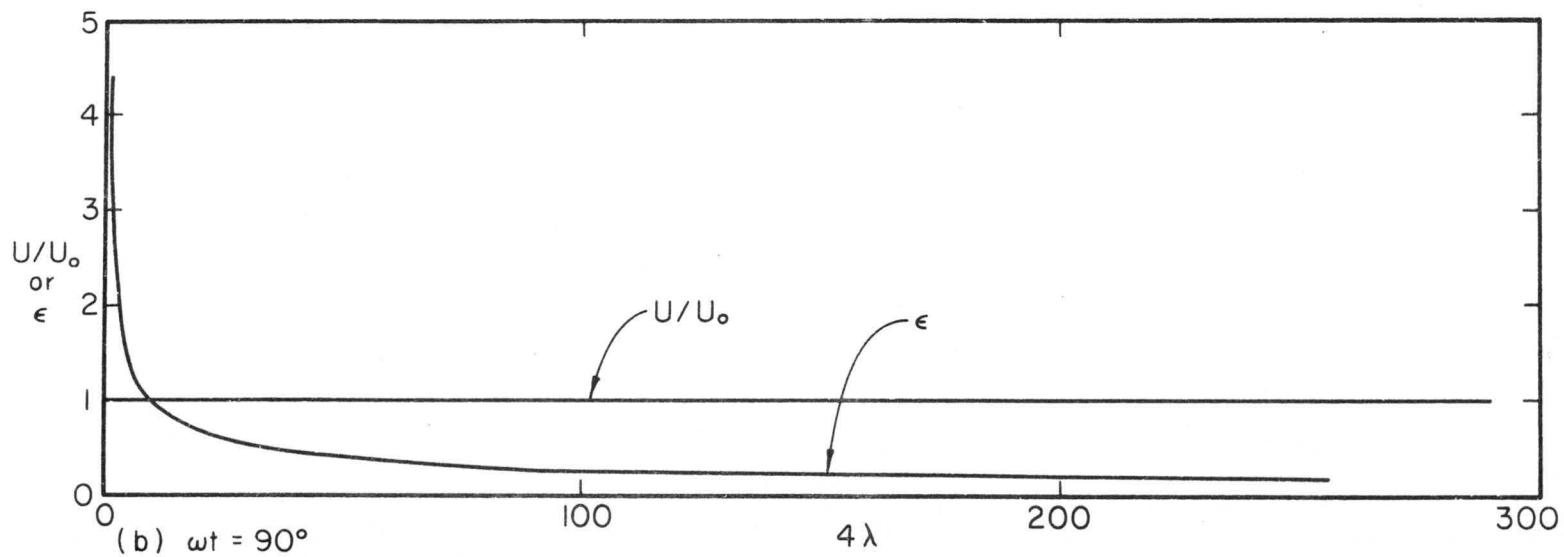
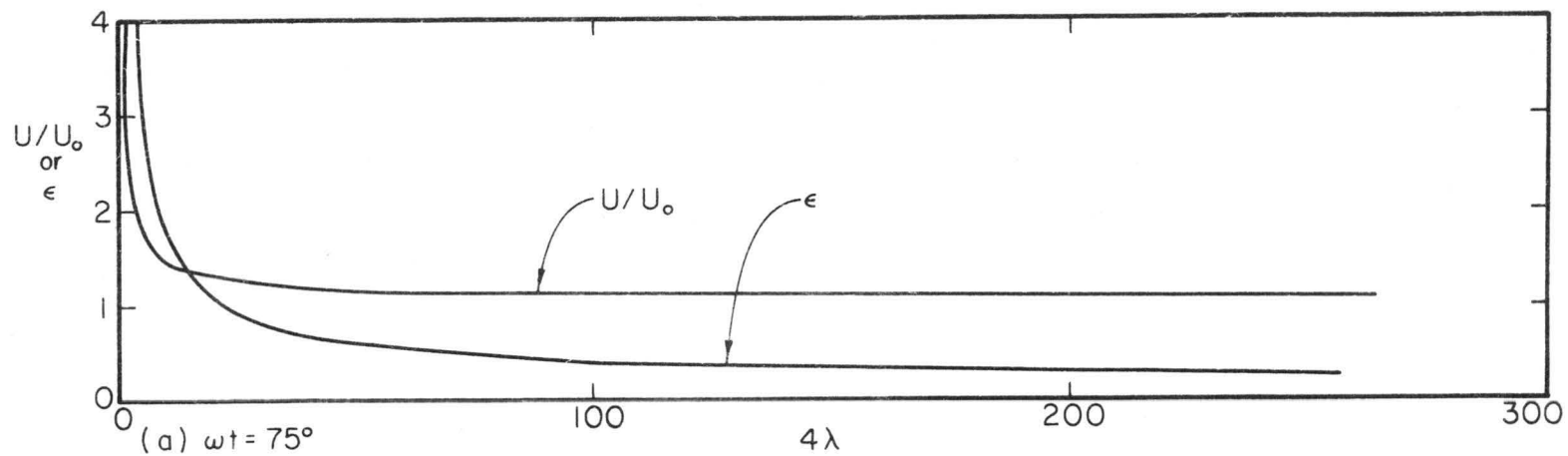


Figure 10 Variations of ϵ and U/U_0 at separation with respect to λ for fluctuating flow past a porous flat plate.

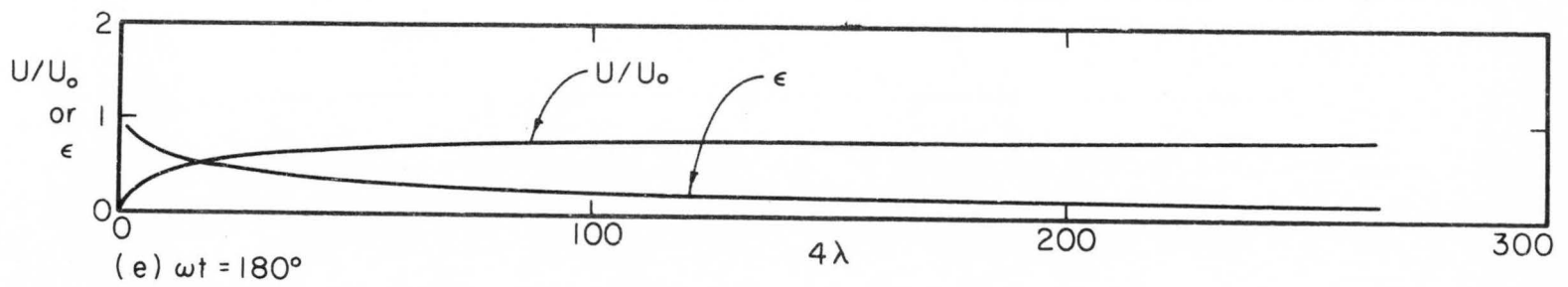
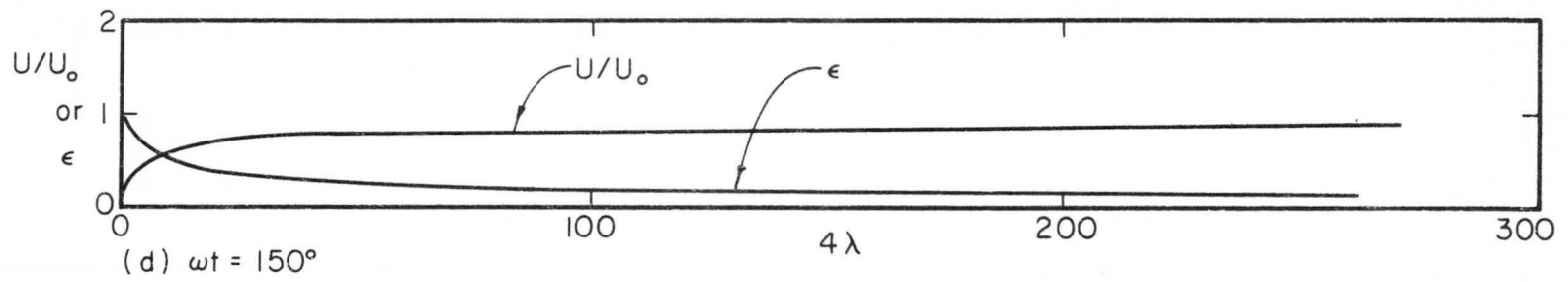
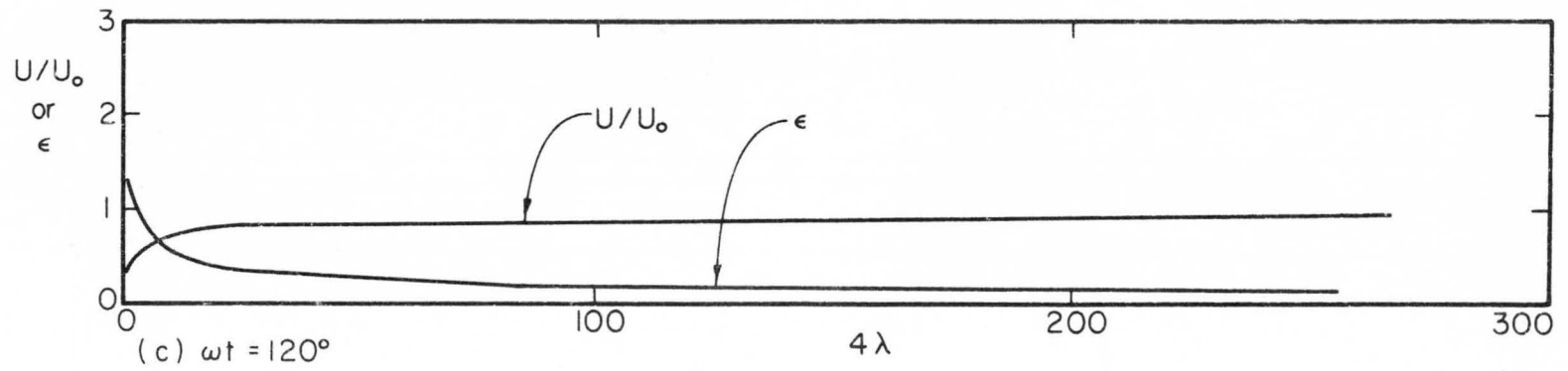


Figure 10 Continued

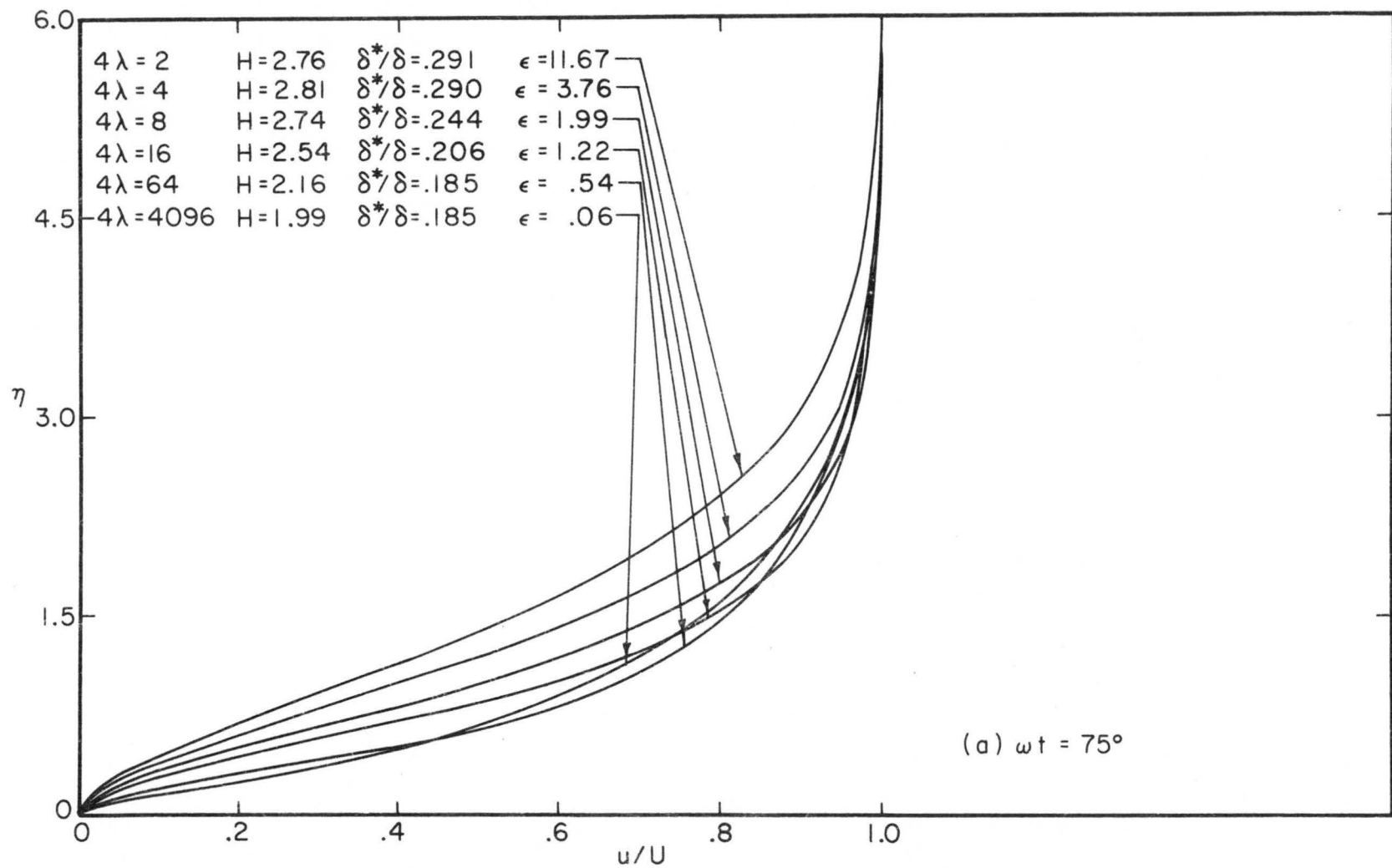


Figure 11 Velocity profiles at separation for fluctuating flow past a porous flat plate.

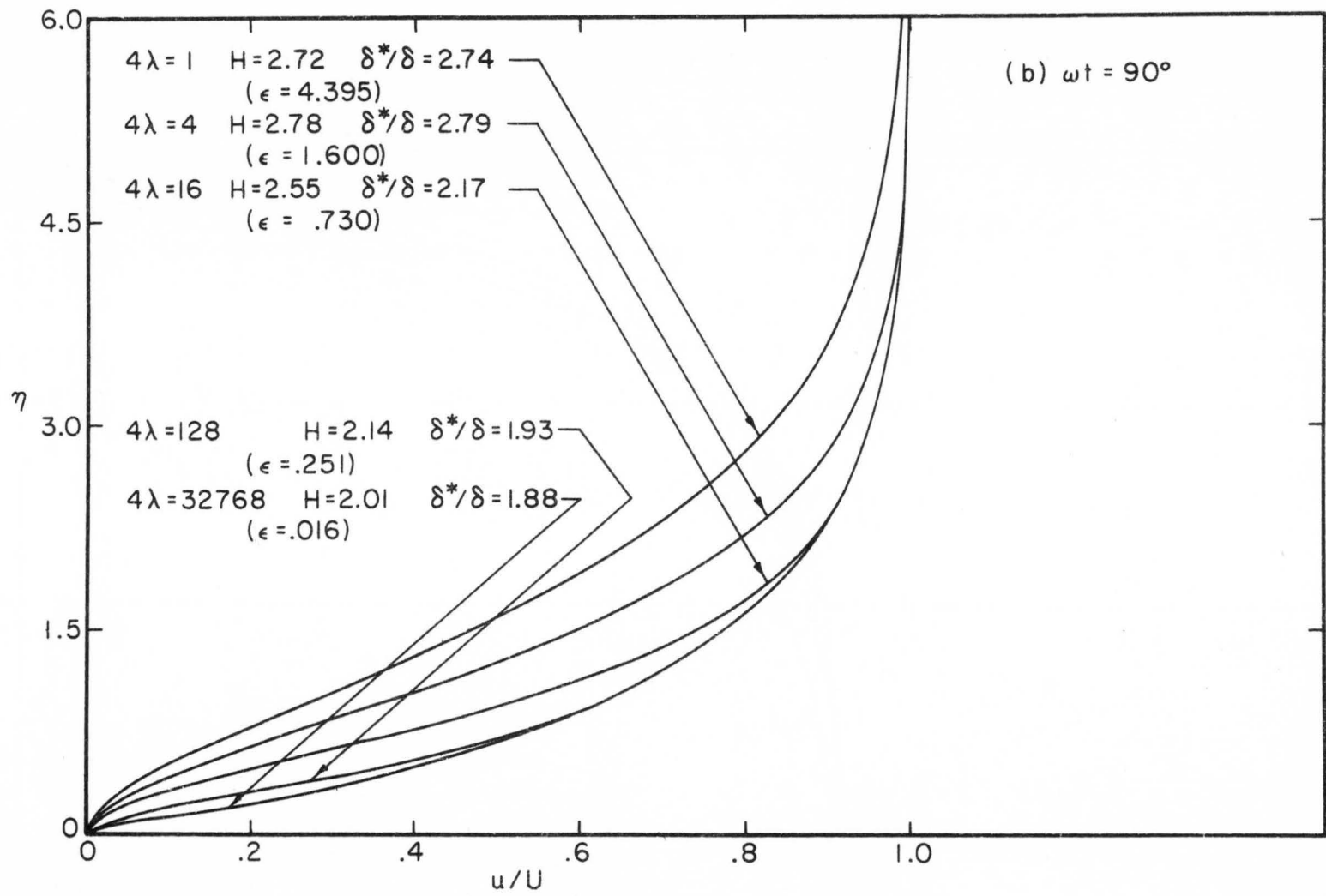


Figure II Continued

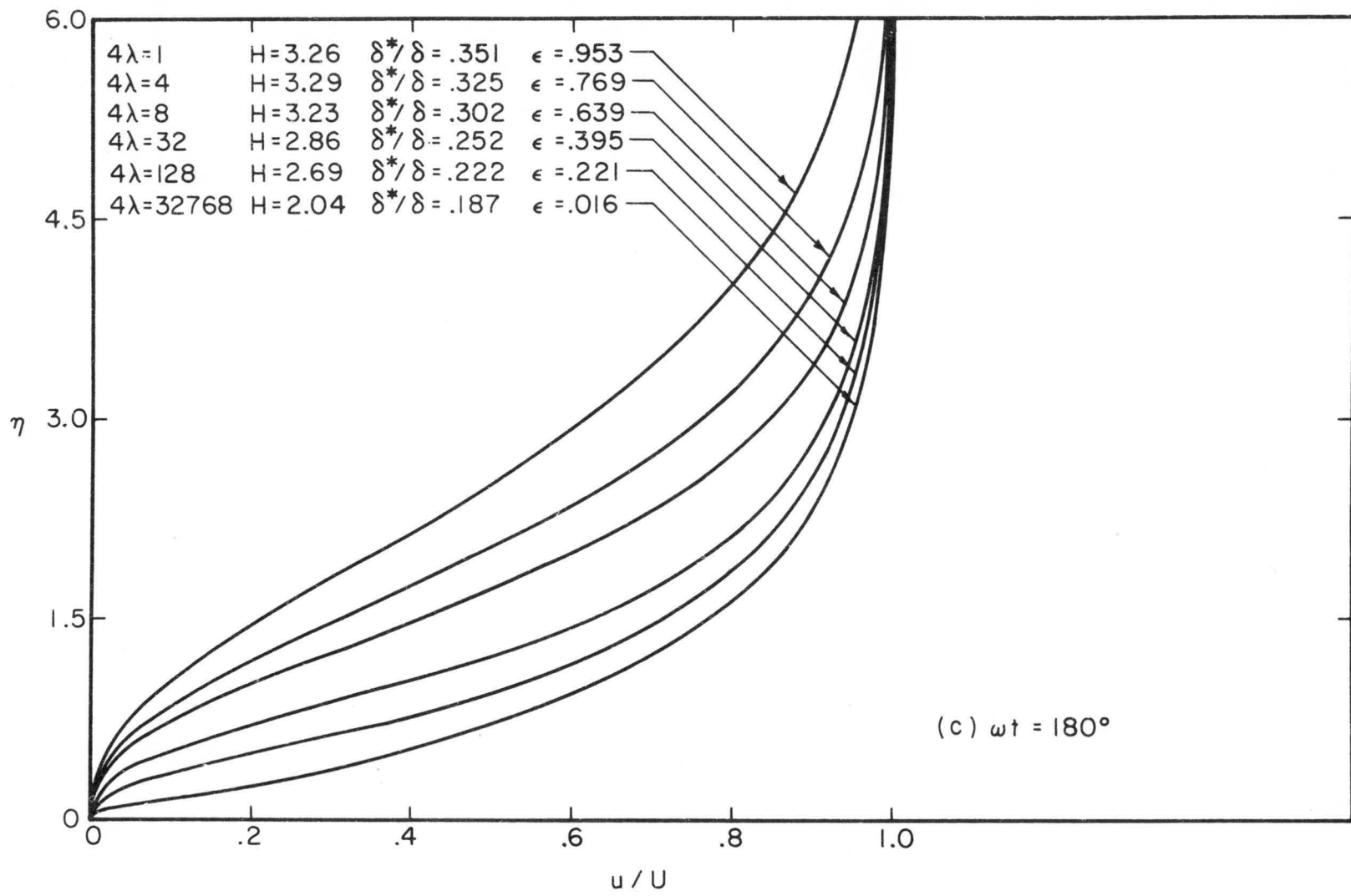


Figure II Continued

$$\begin{aligned}
\frac{\delta^*}{\delta_0^*} &= \int_0^\infty \left(1 - \frac{u}{U}\right) \frac{dy}{\delta_0^*} \\
&= \frac{1}{(1+\epsilon \cos \omega t)} \left\{ -e^{-\eta} \right. \\
&\quad \left. + \epsilon \frac{e^{-h_r \eta} [\cos \omega t (h_i \sinh_i \eta - h_r \cosh_i \eta) - \sin \omega t (h_r \sinh_i \eta + h_i \cosh_i \eta)]}{(h_r)^2 + (h_i)^2} \right\}_0^\infty
\end{aligned} \tag{3-20}$$

where $\delta_0^* = \left| \frac{v}{v_w} \right|$ is the unperturbed displacement thickness

$$\begin{aligned}
\frac{\theta}{\delta_0^*} &= \int_0^\infty \frac{u}{U} \left(1 - \frac{u}{U}\right) \frac{dy}{\delta_0^*} \\
&= \frac{\delta^*}{\delta_0^*} \left\{ \frac{-(h_r+1)\eta}{2\epsilon e} \frac{[h_i \sinh_i \eta - (h_r+1) \cosh_i \eta] \cos \omega t - [(h_r+1) \sinh_i \eta + h_i \cosh_i \eta] \sin \omega t}{(h_r+1)^2 + (h_i)^2} \right. \\
&\quad \left. + \frac{\epsilon^2}{2} \left[\frac{e^{-2h_r \eta} (2h_i \sin 2h_i \eta - 2h_r \cos 2h_i \eta) \cos 2\omega t - (2h_r \sin 2h_i \eta + 2h_i \cos 2h_i \eta) \sin 2\omega t}{(2h_r)^2 + (2h_i)^2} \right. \right. \\
&\quad \left. \left. - \frac{e^{-2h_r \eta}}{2h_r} \right] - \frac{e^{-2\eta}}{2} \right\} \frac{1}{(1+\epsilon \cos \omega t)^2} .
\end{aligned} \tag{3-21}$$

The profile parameters H and δ^*/δ again are calculated by using a computer program. Table 3 contains parts of the computed results. The results are also plotted in Figure 12 together with the empirical relaxed and unrelaxed separation correlation curves. Also, in preparing Figure 12 we have neglected the separation profiles which have the same properties as described in Figure 5.

3.2.2 Comparison with the relaxed and unrelaxed separation correlations - From Figure 12, we can see, for very high frequencies all the correlation curves also appear to terminate at a specific point,

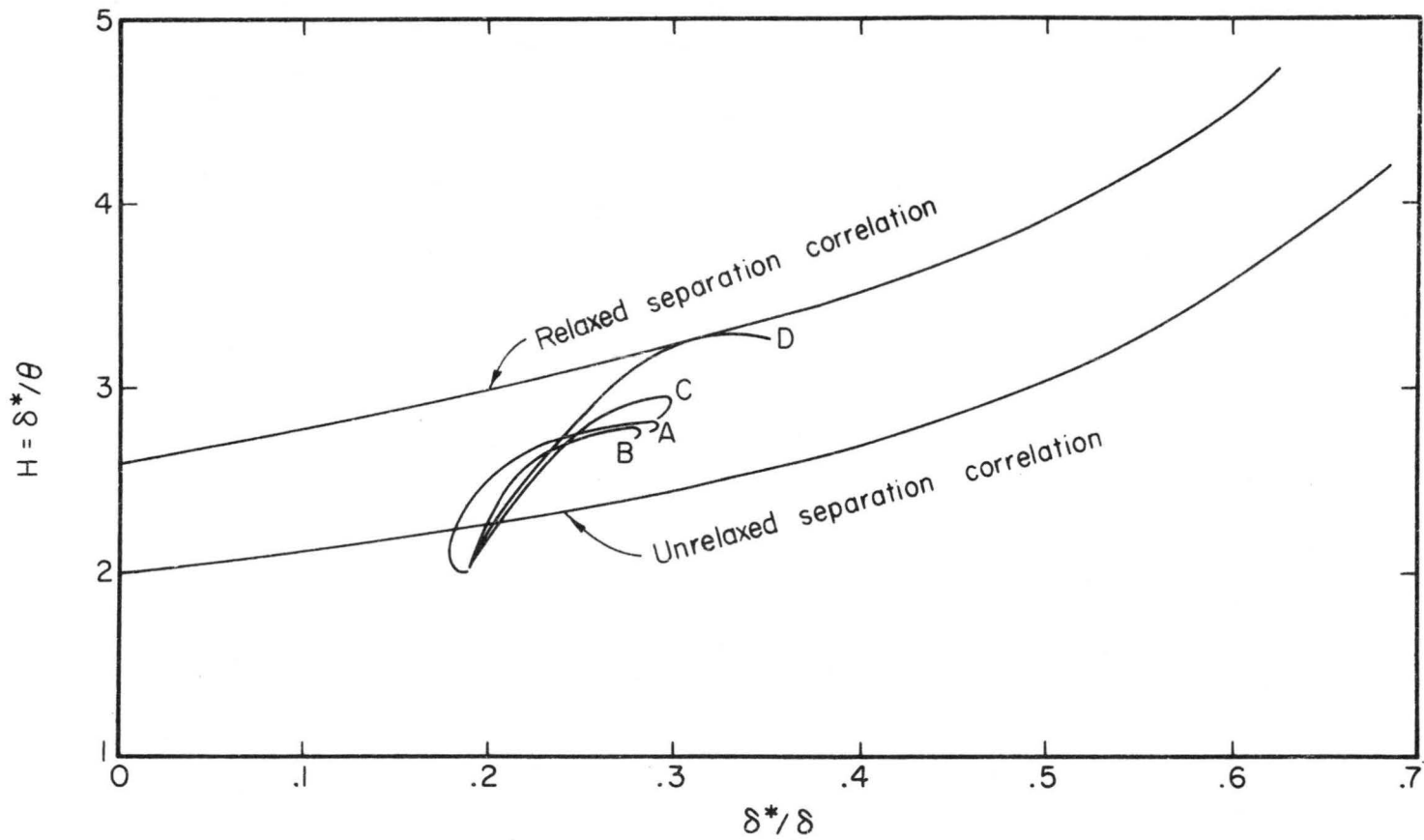


Figure 12 Comparison of separation profile parameters of fluctuating flow past a porous flat plate with the empirical relaxed and unrelaxed separation correlations. A, $\omega t = 75^\circ$; B, $\omega t = 90^\circ$; C, $\omega t = 165^\circ$; D, $\omega t = 180^\circ$.

as in the case of unsteady pipe flow, but now the point is slightly below the empirical unrelaxed correlation curve. As frequencies decrease, these correlation curves pass across the empirical unrelaxed correlation curve and fall in the region between the two separation curves. For very low frequencies these curves approach the relaxed separation curve, but there exists a 'hook' at the end of each curve. Figure 13 shows some separation profiles corresponding to points on the hooks. The appearance of these hooks is not understood at the present time. Stuart's solution thus lends theoretical justification to the unrelaxed separation correlation, and provides more evidence about the importance of the time factor in separation.

Figures 14 and 15 show the variations of the form factor H with respect to the pressure gradient parameters λ_t and λ_θ , respectively. The correlation curves again are diverged at small values of λ_t and λ_θ as in the unsteady pipe flow case. Thus, both results suggest that this may be an important deviation from the separation model of Sandborn (11).

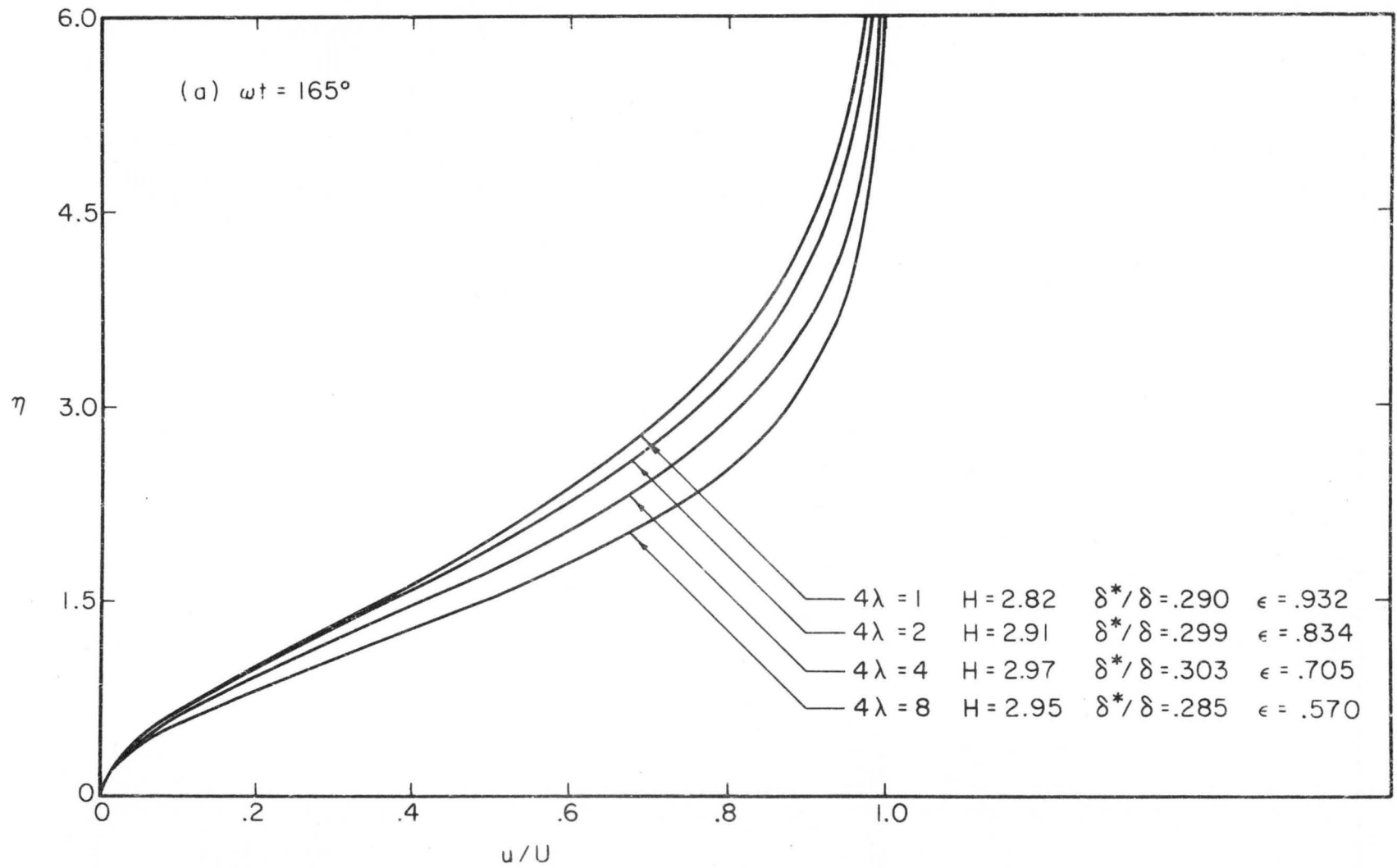


Figure 13 Separation velocity profiles for the points on the hooks

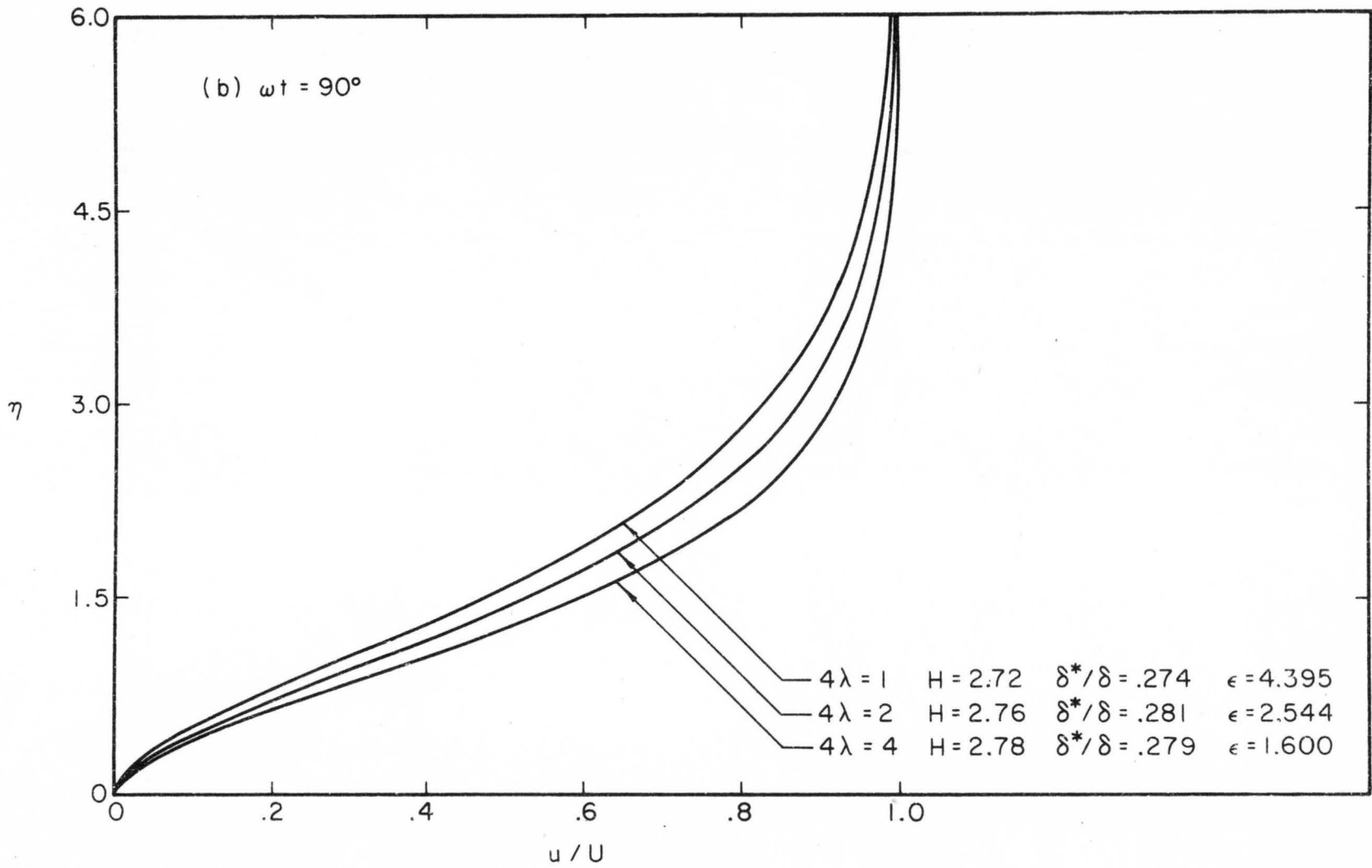


Figure 13 Continued

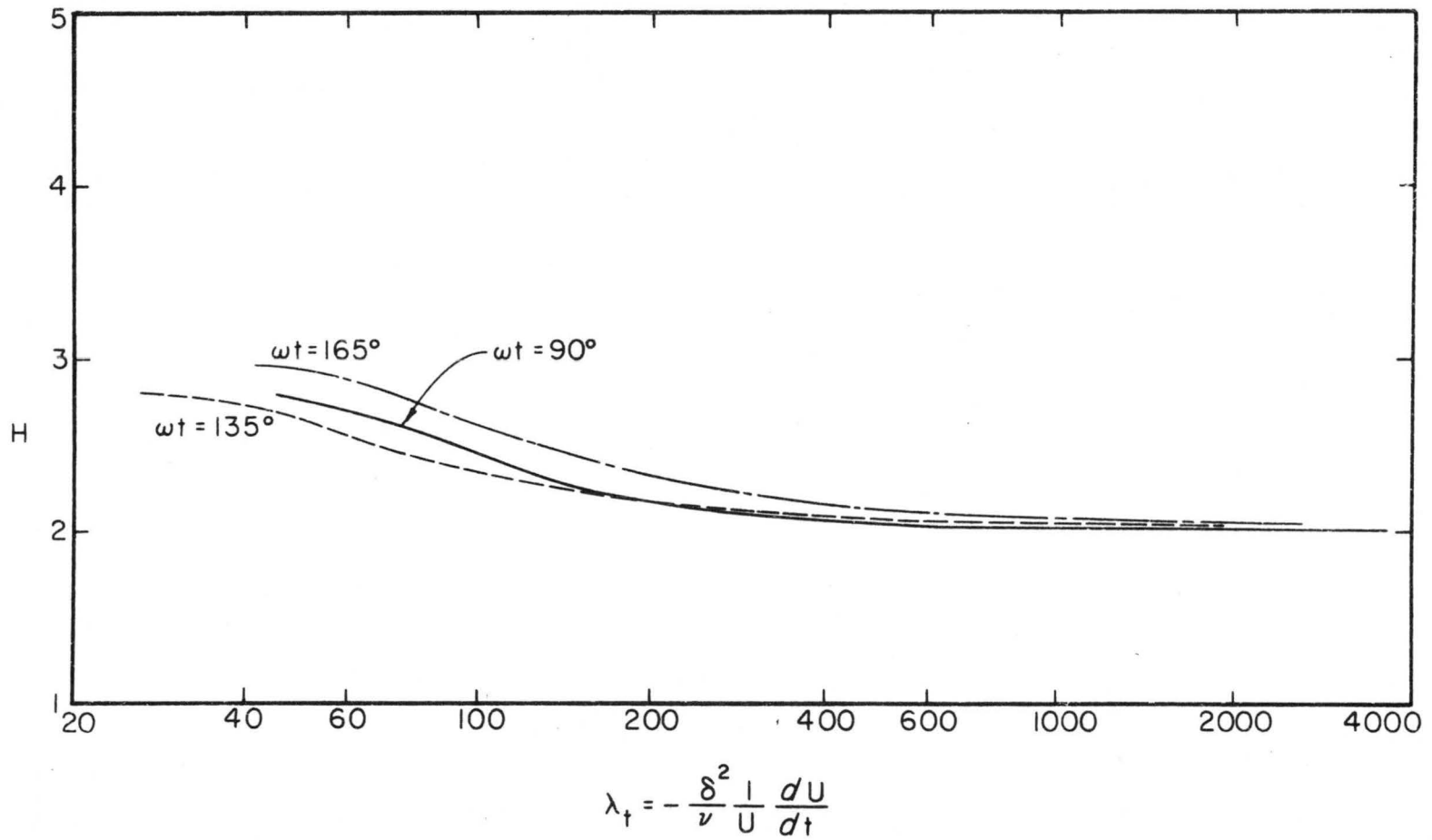


Figure 14 Variations of the form factor at separation with the pressure gradient parameter $-\frac{\delta^2}{\nu} \frac{1}{U} \frac{dU}{dt}$ for fluctuating flow past a porous flat plate.

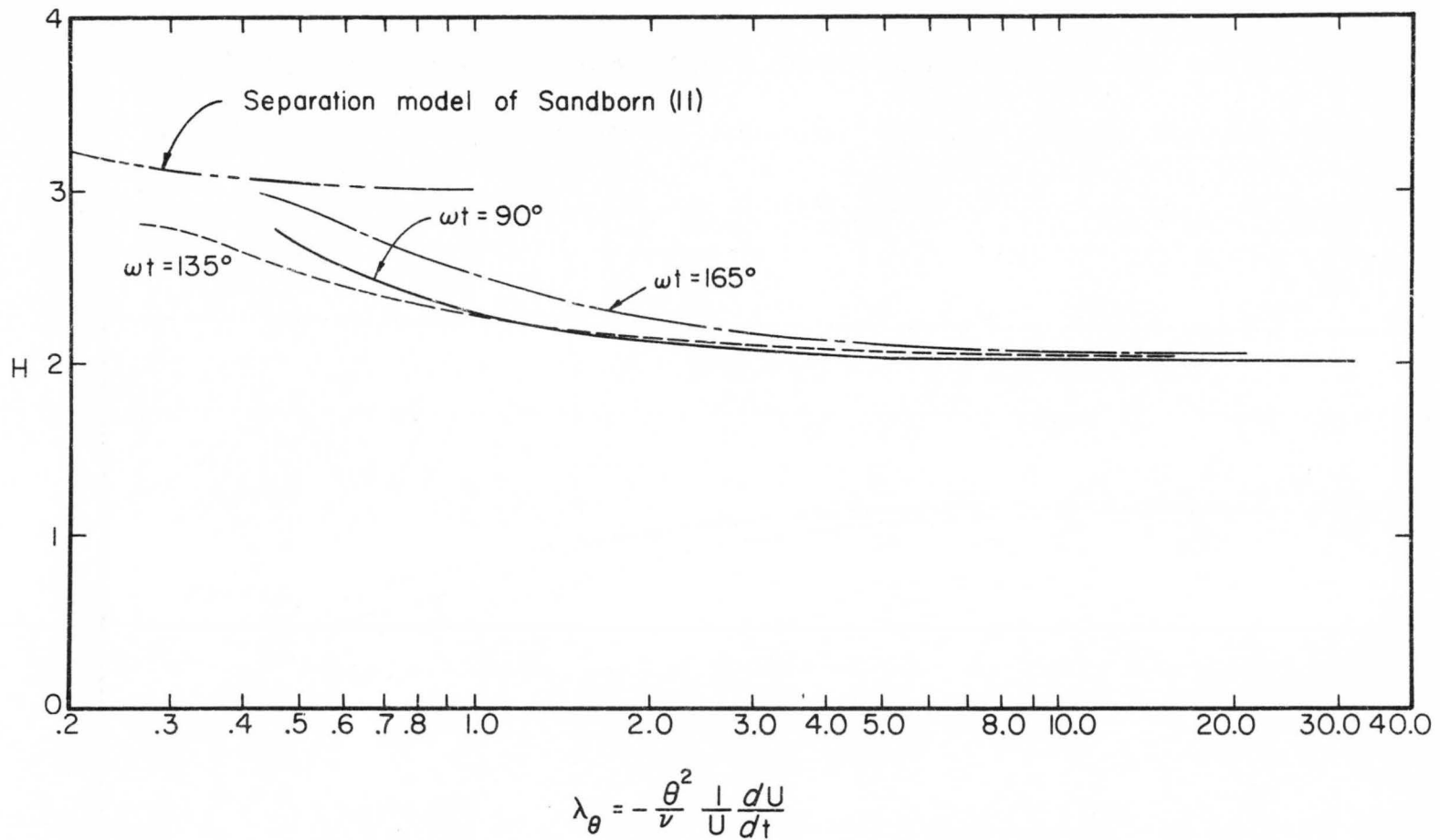


Figure 15 Variations of the form factor at separation with the pressure gradient parameter $-\frac{\theta^2}{\nu} \frac{1}{U} \frac{dU}{dt}$ for fluctuating flow past a porous flat plate.

Chapter IV

CONCLUDING REMARKS

A time varying pipe flow was analyzed. The velocity distributions and velocity profile parameters at separation were computed and compared with the model for relaxed (steady) and unrelaxed (unsteady) separation criteria proposed by Sandborn and Kline.

For very low frequencies, the velocity profile at separation for the unsteady pipe flow agree well with the empirical relaxed separation profile with the same form factor. The separation correlation curves lie slightly below the empirical relaxed separation correlation criterion. For very high frequencies, viscosity does not have time to adjust the velocity to the changes imposed by the exciting pressure-gradient fluctuations across the greater part of the layer. The solved high-frequency separation profile thus resembles the velocity profile for steady flow except in a thin layer near the wall where the effect of viscosity can be felt for the oscillations. The separation correlation curves appear to end at a point on the empirical unrelaxed separation correlation criterion. The present studies thus suggest that the empirical relaxed and unrelaxed correlation curves may be a reasonable approximation, and confirm adjustment time is an important factor for separation to be steady or unsteady.

Stuart's solution for fluctuating flow past an infinite porous flat plate was further analyzed. The solved high-frequency separation correlation curves appear to terminate at a point below the empirical unrelaxed separation correlation curve. The low-frequency separation correlation curves approach the relaxed separation correlation curve,

but bend down slightly at the end. The results also demonstrate adjustment time is important in separation.

Separation criteria in terms of the non-dimensional pressure gradient parameter and the velocity profile form factor are also given for both the unsteady pipe flow and the Stuart's solution. The results show velocity profiles at separation may not be a one parameter family of velocity profiles as implied by the separation model of Sandborn (11). It is suspected that this discrepancy may indicate the dependency on the time history is not adequately expressed by the classical pressure gradient parameter.

BIBLIOGRAPHY

BIBLIOGRAPHY

1. Curle, N., A Two-Parameter Method for Calculating the Two-Dimensional Incompressible Laminar Boundary Layer. Jour. Royal Aeronautical Soc., Vol. 11, p. 117, 1967.
2. Doenhoff, A. E. von and Tetervin, N., Determination of General Relations for the Behavior of Turbulent Boundary Layers. NACA Report 772, 1943.
3. Head, M. R., and Hayasi, N., Approximate Calculations of the Incompressible Laminar Boundary Layer. Aeronautical Quarterly, August 1967.
4. Ito, H., Theory of Laminar Flow Through a Pipe with Non-Steady Pressure Gradient. Rep. Inst. High-Speed Mech., Tohoku Univ., No. 3, p. 163, 1953.
5. Lighthill, M. J., The Response of Laminar Skin Friction and Heat Transfer to Fluctuations in the Stream Velocity. Proc. Royal Soc. A, Vol. 224, p. 1, 1954.
6. Liu, C. Y., Boundary Layer Separation. Ph.D. Dissertation, Colorado State University, Fort Collins, Colorado, 1967.
7. Liu, C. Y., and Sandborn, V. A., Evaluation of the Separation Properties of Laminar Boundary Layers. Aeronautical Quarterly, Vol. XIX, p. 235, 1968.
8. Liu, C. Y., and Sandborn, V. A., Laminar Velocity Profiles in Adverse Pressure Gradients. Journal of Aircraft, Vol. 5, p. 93, 1968.
9. Pohlhausen, K., Zur Waherungsweisen Integration der Laminaren Reibungsschicht. ZAMM 1, p. 252, 1921.
10. Rosenhead, L., Laminar Boundary Layer. Oxford at the Charendou Press, London, 1963.
11. Sandborn, V. A., Characteristics of Boundary Layers at Separation and Reattachment. Research Memorandum No. 14, Department of Civil Engineering, Colorado State University, 1969.
12. Sandborn, V. A., An Equation for the Mean Velocity Distribution of Boundary Layers. NASA Memo 2-5-59E, 1959.
13. Sandborn, V. A., and Kline, S. J., Flow Models in Boundary Layer Stall Inception. Jour. of Basic Engineering, Trans. ASME, Series D, Vol. 83, p. 317, 1961.
14. Sandborn, V. A., and Liu, C. Y., On Turbulent Boundary Layer Separation, Journal of Fluid Mechanics, Vol. 23, p. 293, 1968.

15. Schlichting, H., *Boundary-Layer Theory*. Sixth Edition, McGraw-Hill Publishing Co., N. Y., 1968.
16. Sexl, T., *Über den von E. G. Richardson entdeckten Annulareffekt*. *Z. Phys.* 61, p. 349, 1930.
17. Stratford, B. S., *The Prediction of Separation of the Turbulent Boundary Layer*. *Journal of Fluid Mechanics*, Vol. 5, p. 1, 1959.
18. Stratford, B. S., *An Experimental Flow with Zero Skin Friction Throughout Its Region of Pressure Rise*. *Journal of Fluid Mechanics*, Vol. 5, p. 17, 1959.
19. Stuart, J. T., *A Solution of the Navier-Stokes and Energy Equations Illustrating the Response of Skin Friction and Temperature of an Infinite Plate Thermometer to Fluctuations in the Stream Velocity*. *Proc. Royal Soc. A.*, Vol. 231, p. 116, 1955.
20. Thwaites, B., *Approximate Calculation of the Laminar Boundary Layer*. *Aeronautical Quarterly*, Vol. 1, p. 245, 1949.
21. Wylie, C. R. Jr., *Advanced Engineering Mathematics*. Third Edition, McGraw-Hill Publishing Co., N. Y., 1966.

TABLES

TABLE 1 VARIATIONS WITH X OF BER X, BEI X, BER'X, BEI'X FROM X=0 TO X=80

x	Ber x	Bei x	Ber' x	Bei' x
0	1	0	0	0
1	9.84382E-01	2.49566E-01	-6.24458E-02	4.97397E-01
2	7.51734E-01	9.72292E-01	-4.93067E-01	9.71014E-01
3	-2.21380E-01	1.93759E+00	-1.57985E+00	8.80482E-01
4	-2.56342E+00	2.29269E+00	-3.13465E+00	-4.91137E-01
5	-6.23008E+00	1.16034E-01	-3.84534E+00	-4.35414E+00
6	-8.85832E+00	-7.33475E+00	-2.93080E-01	-1.08462E+01
7	-3.63293E+00	-2.12394E+01	1.27645E+01	-1.60415E+01
8	2.09740E+01	-3.50167E+01	3.83113E+01	-7.66032E+00
9	7.39357E+01	-2.47128E+01	6.56008E+01	3.63994E+01
10	1.38840E+02	5.63705E+01	5.12953E+01	1.35309E+02
11	1.33954E+02	2.57205E+02	-9.42119E+01	2.64119E+02
12	-1.28512E+02	5.46949E+02	-4.72569E+02	2.72670E+02
13	-8.82647E+02	6.46636E+02	-1.04734E+03	-1.92606E+02
14	-2.13128E+03	-1.60938E+02	-1.31609E+03	-1.61609E+03
15	-2.96725E+03	-2.95271E+03	9.10553E+01	-4.08776E+03
16	-6.59497E+02	-8.19071E+03	5.34930E+03	-6.00952E+03
17	9.48445E+03	-1.30873E+04	1.56831E+04	-2.15552E+03
18	3.09623E+04	-7.45434E+03	2.63984E+04	1.68409E+04
19	5.60035E+04	2.85273E+04	1.79336E+04	5.90294E+04
20	4.74894E+04	1.14775E+05	-4.88032E+04	1.11855E+05
21	-7.61557E+04	2.33698E+05	-2.71321E+05	9.65772E+04
22	-4.15521E+05	2.53881E+05	-4.63869E+05	-1.20194E+05
23	-9.53546E+05	-1.52737E+05	-5.45342E+05	-7.79084E+05
24	-1.24183E+06	-1.46040E+06	1.80849E+05	-1.88032E+06
25	9.79772E+03	-3.80879E+06	2.70052E+06	-2.61958E+06
26	4.93575E+06	-5.74444E+06	7.45727E+06	-4.59934E+05
27	1.48935E+07	-2.30784E+06	1.18858E+07	8.94431E+06
28	2.55309E+07	1.57762E+07	6.43694E+06	2.89280E+07
29	1.82477E+07	5.69504E+07	-2.76897E+07	5.21872E+07
30	-4.61176E+07	1.10956E+08	-1.09599E+08	4.32922E+07
31	-2.12456E+08	1.07975E+08	-2.22436E+08	-7.63424E+07
32	-4.61092E+08	-1.13201E+08	-2.38742E+08	-4.04349E+08
33	-5.53103E+08	-7.70090E+08	1.61924E+08	-9.24955E+08
34	1.59559E+08	-1.88756E+09	1.44532E+09	-1.19396E+09
35	2.69363E+09	-2.66087E+09	3.74773E+09	6.15699E+07
36	7.55140E+09	-5.45406E+08	5.62995E+09	4.96213E+09
37	1.21922E+10	8.98464E+09	2.10194E+09	1.48531E+10
38	6.86654E+09	2.95191E+10	-1.61104E+10	2.53388E+10
39	-2.79417E+10	5.38524E+10	-5.74805E+10	1.76264E+10
40	-1.12597E+11	4.56281E+10	-1.10471E+11	-4.79332E+10
41	-2.30841E+11	-7.70498E+10	-1.05915E+11	-2.16781E+11
42	-2.51327E+11	-4.17869E+11	1.20789E+11	-4.68210E+11
43	1.61180E+11	-9.64965E+11	7.93763E+11	-5.56392E+11
44	1.50121E+12	-1.25925E+12	1.93487E+12	1.85531E+11

TABLE 1 VARIATIONS WITH X OF BER X, BEI X,
BER'X, BEI'X FROM X=0 TO X=80 - Cont'd.

x	Ber x	Bei x	Ber' x	Bei' x
45	3.92920E+12	3.60867E+10	2.70902E+12	2.80366E+12
46	5.94457E+12	5.71537E+12	4.78823E+11	7.80677E+12
47	2.32111E+12	1.56422E+13	-9.44489E+12	1.25351E+13
48	-1.68525E+13	2.68901E+13	-3.07555E+13	6.81581E+12
49	-6.07815E+13	1.90564E+13	-5.58322E+13	-2.97016E+13
50	-1.17624E+14	-5.01926E+13	-4.65989E+13	-1.18165E+14
51	-1.14082E+14	-2.30071E+14	8.31471E+13	-2.41093E+14
52	1.26012E+14	-5.00145E+14	4.41561E+14	-2.59722E+14
53	8.45158E+14	-5.99346E+14	1.01343E+15	1.79516E+14
54	2.07324E+15	1.87717E+14	1.31400E+15	1.59706E+15
55	2.92222E+15	2.99342E+15	-7.70891E+13	4.15578E+15
56	5.56413E+14	8.38943E+15	-5.54401E+15	6.25054E+15
57	-1.01058E+16	1.35474E+16	-1.66367E+16	2.31409E+15
58	-3.31407E+16	7.50677E+15	-2.84558E+16	-1.81918E+16
59	-6.04675E+16	-3.18174E+16	-1.97438E+16	-6.49864E+16
60	-5.08780E+16	-1.27647E+17	5.49125E+16	-1.25171E+17
61	8.89990E+16	-2.61668E+17	2.47234E+17	-1.19942E+17
62	4.78075E+17	-2.83862E+17	5.34911E+17	1.39637E+17
63	1.10224E+18	1.90697E+17	6.35783E+17	9.12753E+17
64	1.43683E+18	1.73257E+18	-2.20418E+17	2.22756E+18
65	-6.69167E+16	4.52912E+18	-3.24947E+18	3.12032E+18
66	-6.02433E+18	6.84241E+18	-9.05254E+18	5.26377E+17
67	-1.81664E+19	2.59279E+18	-1.45431E+19	-1.10320E+19
68	-3.11933E+19	-1.97903E+19	-7.83285E+18	-3.59056E+19
69	-2.18594E+19	-7.10906E+19	3.49718E+19	-6.52095E+19
70	5.95318E+19	-1.37417E+20	1.38840E+20	-5.40880E+19
71	2.70911E+20	-1.32493E+20	2.83339E+20	9.88166E+19
72	5.88129E+20	1.51595E+20	3.04578E+20	5.22020E+20
73	7.02194E+20	1.00169E+21	-2.16613E+20	1.19796E+21
74	-2.35511E+20	2.45285E+21	-1.89940E+21	1.55128E+21
75	-3.57076E+21	3.44836E+21	-4.93944E+21	-1.09645E+20
76	-9.98254E+21	6.08006E+20	-7.42285E+21	-6.63296E+21
77	-1.60867E+22	-1.21352E+22	-2.68901E+21	-1.98772E+22
78	-8.75774E+21	-3.96497E+22	2.19001E+22	-3.39747E+22
79	3.84893E+22	-7.22095E+22	7.80311E+22	-2.33839E+22
80	1.53509E+23	-6.02449E+22	1.50182E+23	6.63276E+22

In calculating the functions Ber x, Bei x, Ber' x, and Bei' x, the number of terms used in each infinitive series depends on the values of x, but in each case the truncation error is less than 0.000001 %.

TABLE 2 VARIATIONS OF δ^*/R , θ/R , H , AND ϵ WITH
RESPECT TO $\sqrt{\frac{\omega}{\nu}} R$ FOR TIME VARYING PIPE FLOW

ωt		$\frac{3}{4} \pi$	π	$\frac{7}{6} \pi$	$\frac{4}{3} \pi$	$\frac{3}{2} \pi$
$\sqrt{\frac{\omega}{\nu}} R$						
0.4	δ^*/R	0.467	0.477	0.466	0.466	0.467
	θ/R	0.127	0.127	0.127	0.127	0.127
	H	3.672	3.770	3.664	3.668	3.669
	ϵ	1.444	1.001	1.142	1.934	50.037
1.2	δ^*/R	0.468	0.477	0.455	0.463	0.466
	θ/R	0.127	0.127	0.127	0.127	0.127
	H	3.684	3.769	3.570	3.642	3.661
	ϵ	1.792	1.042	1.092	1.595	5.885
2.0	δ^*/R	0.467	0.476	0.516	0.443	0.459
	θ/R	0.127	0.127	0.122	0.127	0.127
	H	3.672	3.759	4.228	3.490	3.607
	ϵ	3.297	1.292	1.187	1.459	2.899
3.2	δ^*/R	0.452	0.469	0.485	0.556	0.396
	θ/R	0.127	0.127	0.126	0.112	0.121
	H	3.556	3.702	3.862	4.970	3.247
	ϵ	12.380	2.169	1.746	1.884	2.883
4.8	δ^*/R	0.392	0.442	0.464	0.499	0.710
	θ/R	0.121	0.126	0.126	0.122	0.025
	H	3.235	3.512	3.696	4.085	27.960
	ϵ	30.872	3.380	2.623	2.743	3.999
6.4	δ^*/R	0.295	0.402	0.431	0.465	0.552
	θ/R	0.095	0.122	0.124	0.122	0.103
	H	3.097	3.285	3.480	3.797	5.363
	ϵ	54.424	4.508	3.448	3.565	5.106
8.0	δ^*/R	0.127	0.371	0.401	0.432	0.495
	θ/R	0.065	0.120	0.122	0.121	0.111
	H	3.328	3.104	3.296	3.568	4.473
	ϵ	86.394	5.644	4.276	4.388	6.218
10.0	δ^*/R	0.179	0.354	0.380	0.404	0.450
	θ/R	0.058	0.121	0.122	0.121	0.113
	H	3.074	2.923	3.115	3.350	3.966
	ϵ	136.278	7.061	5.311	5.421	7.619

TABLE 2 VARIATIONS OF δ^*/R , θ/R , H, AND ϵ WITH RESPECT
TO $\sqrt{\frac{\omega}{\nu}} R$ FOR TIME VARYING PIPE FLOW - Continued

$\sqrt{\frac{\omega}{\nu}} R$	ωt	$\sqrt{\frac{\omega}{\nu}} R$				
		$\frac{3}{4} \pi$	π	$\frac{7}{6} \pi$	$\frac{4}{3} \pi$	$\frac{3}{2} \pi$
16.0	δ^*/R	0.140	0.342	0.359	0.375	0.399
	θ/R	0.061	0.128	0.127	0.125	0.121
	H	2.279	2.673	2.833	2.991	3.301
	ϵ	353.879	11.308	8.417	8.522	11.843
24.0	δ^*/R	0.115	0.337	0.350	0.360	0.375
	θ/R	0.061	0.131	-0.129	0.128	0.125
	H	1.897	2.578	2.700	2.809	2.996
	ϵ	802.420	16.967	12.558	12.660	17.490
40.0	δ^*/R	0.096	0.335	0.343	0.349	0.358
	θ/R	0.061	0.132	0.131	0.130	0.129
	H	1.579	2.527	2.608	2.676	2.781
	ϵ	2242.570	28.282	20.840	20.941	28.796
80.0	δ^*/R	0.081	0.334	0.338	0.341	0.345
	θ/R	0.061	0.133	0.133	0.132	0.131
	H	1.337	2.504	2.549	2.583	2.633
	ϵ	9073.181	56.566	41.544	41.642	57.070

TABLE 3 VARIATIONS OF SEPARATION PROFILE PARAMETERS FOR
FLUCTUATING FLOW PAST A POROUS FLAT PLATE

ωt			75°	$\pi/2$	120°	165°	π
4λ							
2	δ/δ_o^*	5.500	6.000	6.500	7.300	7.700	
	δ^*/δ_o^*	1.599	1.689	1.834	2.184	2.568	
	θ/δ_o^*	0.576	0.612	0.664	0.750	0.782	
	H	2.775	2.758	2.764	2.913	3.284	
	δ^*/δ	0.291	0.281	0.282	0.299	0.333	
4	δ/δ_o^*	4.700	5.300	5.900	6.500	6.900	
	δ^*/δ_o^*	1.364	1.476	1.643	1.970	2.245	
	θ/δ_o^*	0.485	0.532	0.590	0.662	0.682	
	H	2.810	2.776	2.786	2.974	3.293	
	δ^*/δ	0.290	0.279	0.278	0.303	0.325	
8	δ/δ_o^*	4.800	5.300	5.700	6.100	6.400	
	δ^*/δ_o^*	1.173	1.295	1.460	1.737	1.935	
	θ/δ_o^*	0.428	0.479	0.533	0.588	0.600	
	H	2.737	2.703	2.737	2.954	3.225	
	δ^*/δ	0.244	0.244	0.256	0.285	0.302	
16	δ/δ_o^*	5.100	5.400	5.600	5.900	6.100	
	δ^*/δ_o^*	1.052	1.170	1.317	1.539	1.681	
	θ/δ_o^*	0.415	0.460	0.503	0.541	0.548	
	H	2.538	2.544	2.618	2.846	3.068	
	δ^*/δ	0.206	0.217	0.235	0.261	0.276	
32	δ/δ_o^*	5.200	5.300	5.500	5.700	5.900	
	δ^*/δ_o^*	0.989	1.092	1.215	1.386	1.488	
	θ/δ_o^*	0.426	0.460	0.491	0.515	0.520	
	H	2.322	2.373	2.473	2.690	2.863	
	δ^*/δ	0.190	0.206	0.221	0.243	0.252	

TABLE 3 VARIATIONS OF SEPARATION PROFILE PARAMETERS FOR FLUCTUATING FLOW PAST A POROUS FLAT PLATE - Continued

4λ	ωt	75°	$\pi/2$	120°	165°	π
64	δ/δ_o^*	5.200	5.300	5.500	5.600	5.700
	δ^*/δ_o^*	0.961	1.047	1.145	1.274	1.346
	θ/δ_o^*	0.445	0.469	0.489	0.503	0.506
	H	2.161	2.234	2.341	2.531	2.663
	δ^*/δ	0.185	0.198	0.208	0.227	0.236
128	δ/δ_o^*	5.300	5.300	5.400	5.500	5.600
	δ^*/δ_o^*	0.954	1.023	1.097	1.192	1.244
	θ/δ_o^*	0.463	0.478	0.490	0.498	0.499
	H	2.061	2.140	2.240	2.394	2.491
	δ^*/δ	0.180	0.193	0.203	0.217	0.222
256	δ/δ_o^*	5.300	5.300	5.400	5.500	5.500
	δ^*/δ_o^*	0.957	1.009	1.066	1.135	1.172
	θ/δ_o^*	0.476	0.485	0.492	0.496	0.497
	H	2.010	2.082	2.167	2.287	2.358
	δ^*/δ	0.181	0.190	0.197	0.206	0.213
512	δ/δ_o^*	5.300	5.300	5.400	5.400	5.500
	δ^*/δ_o^*	0.963	1.002	1.044	1.094	1.120
	θ/δ_o^*	0.484	0.489	0.493	0.495	0.496
	H	1.988	2.049	2.117	2.208	2.259
	δ^*/δ	0.182	0.189	0.193	0.203	0.204
2048	δ/δ_o^*	5.300	5.300	5.400	5.400	5.400
	δ^*/δ_o^*	0.976	0.997	1.019	1.045	1.058
	θ/δ_o^*	0.497	0.493	0.495	0.495	0.495
	H	1.983	2.021	2.060	2.109	2.135
	δ^*/δ	0.184	0.188	0.189	0.193	0.196

TABLE 3 VARIATIONS OF SEPARATION PROFILE PARAMETERS FOR FLUCTUATING FLOW PAST A POROUS FLAT PLATE - Continued

4λ \ / \ ωt		75°	$\pi/2$	120°	165°	π
8192	δ/δ_0^*	5.300	5.300	5.400	5.400	5.400
	δ^*/δ_0^*	0.985	0.995	1.007	1.020	1.027
	θ/δ_0^*	0.494	0.495	0.495	0.495	0.495
	H	1.992	2.013	2.033	2.059	2.072
	δ^*/δ	0.186	1.188	0.186	0.189	0.190
32768	δ/δ_0^*	5.300	5.300	5.400	5.400	5.400
	δ^*/δ_0^*	0.990	0.995	1.001	1.008	1.011
	θ/δ_0^*	0.495	0.495	0.495	0.495	0.495
	H	2.000	2.011	2.021	2.034	2.041
	δ^*/δ	0.187	0.188	0.186	0.187	0.187

DOCUMENT CONTROL DATA - R&D

(Security classification of title, body of abstract and indexing annotation must be entered when the overall report is classified)

1. ORIGINATING ACTIVITY (Corporate author) Fluid Dynamics and Diffusion Laboratory College of Engineering, Colorado State University Fort Collins, Colorado 80521		2a. REPORT SECURITY CLASSIFICATION Unclassified	
		2b. GROUP	
3. REPORT TITLE Flow Separation in Time Varying Flow			
4. DESCRIPTIVE NOTES (Type of report and inclusive dates) Technical Report			
5. AUTHOR(S) (Last name, first name, initial) Chow, Fan-Kuo and Sandborn, V. A.			
6. REPORT DATE December 1969		7a. TOTAL NO. OF PAGES 62	7b. NO. OF REFS 21
8a. CONTRACT OR GRANT NO. N00014-68-A-0493 b. PROJECT NO. NR 062-414/6-6-68(Code 438) c. d.		9a. ORIGINATOR'S REPORT NUMBER(S) CER69-70FkC-VAS23 9b. OTHER REPORT NO(S) (Any other numbers that may be assigned this report)	
10. AVAILABILITY/LIMITATION NOTICES Distribution of this report is unlimited			
11. SUPPLEMENTARY NOTES		12. SPONSORING MILITARY ACTIVITY Office of Naval Research U. S. Department of Defense Washington, D.C.	
13. ABSTRACT An exact solution of time varying pipe flow with a fluctuating velocity superimposed on the mean flow is analyzed. The velocity profiles, together with the profile parameters at separation, are computed from a computer program. The results are compared with the model for relaxed (steady) and unrelaxed (unsteady) separation criteria proposed by V. A. Sandborn and S. J. Kline. For very low frequencies, the correlation curves appear to have a reasonable agreement with the proposed relaxed separation criterion. For high frequencies, the correlation curves have been found to fall approximately on the unrelaxed separation criterion. This result demonstrates further that adjustment time is an important factor for separation to be relaxed or unrelaxed, a new concept proposed by Sandborn. In addition, J. T. Stuart's solution for the flow along an infinite flat plate with normal suction and periodic external velocity is further analyzed. The results again prove to agree with the proposed new concept.			

14. KEY WORDS	LINK A		LINK B		LINK C	
	ROLE	WT	ROLE	WT	ROLE	WT
Flow Separation Time Varying Pipe Flow Velocity Profiles Profile Parameters						

INSTRUCTIONS

1. **ORIGINATING ACTIVITY:** Enter the name and address of the contractor, subcontractor, grantee, Department of Defense activity or other organization (*corporate author*) issuing the report.

2a. **REPORT SECURITY CLASSIFICATION:** Enter the overall security classification of the report. Indicate whether "Restricted Data" is included. Marking is to be in accordance with appropriate security regulations.

2b. **GROUP:** Automatic downgrading is specified in DoD Directive 5200.10 and Armed Forces Industrial Manual. Enter the group number. Also, when applicable, show that optional markings have been used for Group 3 and Group 4 as authorized.

3. **REPORT TITLE:** Enter the complete report title in all capital letters. Titles in all cases should be unclassified. If a meaningful title cannot be selected without classification, show title classification in all capitals in parenthesis immediately following the title.

4. **DESCRIPTIVE NOTES:** If appropriate, enter the type of report, e.g., interim, progress, summary, annual, or final. Give the inclusive dates when a specific reporting period is covered.

5. **AUTHOR(S):** Enter the name(s) of author(s) as shown on or in the report. Enter last name, first name, middle initial. If military, show rank and branch of service. The name of the principal author is an absolute minimum requirement.

6. **REPORT DATE:** Enter the date of the report as day, month, year; or month, year. If more than one date appears on the report, use date of publication.

7a. **TOTAL NUMBER OF PAGES:** The total page count should follow normal pagination procedures, i.e., enter the number of pages containing information.

7b. **NUMBER OF REFERENCES:** Enter the total number of references cited in the report.

8a. **CONTRACT OR GRANT NUMBER:** If appropriate, enter the applicable number of the contract or grant under which the report was written.

8b, 8c, & 8d. **PROJECT NUMBER:** Enter the appropriate military department identification, such as project number, subproject number, system numbers, task number, etc.

9a. **ORIGINATOR'S REPORT NUMBER(S):** Enter the official report number by which the document will be identified and controlled by the originating activity. This number must be unique to this report.

9b. **OTHER REPORT NUMBER(S):** If the report has been assigned any other report numbers (*either by the originator or by the sponsor*), also enter this number(s).

10. **AVAILABILITY/LIMITATION NOTICES:** Enter any limitations on further dissemination of the report, other than those imposed by security classification, using standard statements such as:

- (1) "Qualified requesters may obtain copies of this report from DDC."
- (2) "Foreign announcement and dissemination of this report by DDC is not authorized."
- (3) "U. S. Government agencies may obtain copies of this report directly from DDC. Other qualified DDC users shall request through _____."
- (4) "U. S. military agencies may obtain copies of this report directly from DDC. Other qualified users shall request through _____."
- (5) "All distribution of this report is controlled. Qualified DDC users shall request through _____."

If the report has been furnished to the Office of Technical Services, Department of Commerce, for sale to the public, indicate this fact and enter the price, if known.

11. **SUPPLEMENTARY NOTES:** Use for additional explanatory notes.

12. **SPONSORING MILITARY ACTIVITY:** Enter the name of the departmental project office or laboratory sponsoring (*paying for*) the research and development. Include address.

13. **ABSTRACT:** Enter an abstract giving a brief and factual summary of the document indicative of the report, even though it may also appear elsewhere in the body of the technical report. If additional space is required, a continuation sheet shall be attached.

It is highly desirable that the abstract of classified reports be unclassified. Each paragraph of the abstract shall end with an indication of the military security classification of the information in the paragraph, represented as (TS), (S), (C), or (U).

There is no limitation on the length of the abstract. However, the suggested length is from 150 to 225 words.

14. **KEY WORDS:** Key words are technically meaningful terms or short phrases that characterize a report and may be used as index entries for cataloging the report. Key words must be selected so that no security classification is required. Identifiers, such as equipment model designation, trade name, military project code name, geographic location, may be used as key words but will be followed by an indication of technical context. The assignment of links, rules, and weights is optional.

February 1969

APPROVED DISTRIBUTION LIST FOR UNCLASSIFIED TECHNICAL
REPORTS ISSUED UNDER CONTRACT N00014-68-A-0493-0001
NR 062-414

Technical Library, Building 313
Aberdeen Proving Ground
Aberdeen, Maryland 21005

Dr. F. D. Bennett
Exterior Ballistics Laboratory
Ballistics Research Laboratories
Aberdeen Proving Ground
Aberdeen, Maryland 21005

Mr. C. C. Hudson
Sandia Corporation
Sandia Base
Albuquerque, New Mexico 87115

Defense Documentation Center
Cameron Station
Alexandria, Virginia 22314 (20)

Professor Bruce Johnson
Engineering Department
Naval Academy
Annapolis, Maryland 21402

Library
Naval Academy
Annapolis, Maryland 21402

Professor W. W. Willmarth
Department of Aerospace Engineering
University of Michigan
Ann Arbor, Michigan 48108

Professor A. Kuethe
Department of Aeronautical Engineering
University of Michigan
Ann Arbor, Michigan 48108

AFOSR (SREM)
1400 Wilson Boulevard
Arlington, Virginia 22209

Dr. J. Menkes
Institute for Defense Analyses
400 Army-Navy Drive
Arlington, Virginia 22204

M. J. Thompson
Defense Research Laboratory
University of Texas
P. O. Box 8029
Austin, Texas 78712

Library
Aerojet-General Corporation
6352 N. Irwindale Avenue
Azusa, California 91702

Professor S. Corrsin
Department of Mechanics
Johns Hopkins University
Baltimore, Maryland 21218

Professor M. V. Morkovin
Aeronautics Building
Johns Hopkins University
Baltimore, Maryland 21218

Professor O. M. Phillips
Division of Mechanical Engineering
Institute for Cooperative Research
Johns Hopkins University
Baltimore, Maryland 21218

Geophysical Research Library
Air Force Cambridge Research Center
Bedford, Massachusetts 01731

Librarian
Department of Naval Architecture
University of California
Berkeley, California 94720

Professor Paul Lieber
Department of Mechanical Engineering
University of California
Berkeley, California 94720

Professor J. Johnson
412 Hesse Hall
University of California
Berkeley, California 94720

Professor A. K. Oppenheim
Division of Mechanical Engineering
University of California
Berkeley, California 94720

Professor M. Holt
Division of Aeronautical Sciences
University of California
Berkeley, California 94720

Dr. L. Talbot
Department of Engineering
Berkeley, California 94720

Professor R. J. Emrich
Department of Physics
Lehigh University
Bethlehem, Pennsylvania 18015

Engineering Library
Plant 25
Grumman Aircraft Engineering Corporation
Bethpage, Long Island, New York 11714

Mr. Eugene F. Baird
Chief of Dynamic Analysis
Grumman Aircraft Engineering Corporation
Bethpage, Long Island, New York 11714

Library
Naval Weapons Center
China Lake, California 93555

Library MS 60-3
NASA Lewis Research Center
21000 Brookpark Road
Cleveland, Ohio 44133

Professor J. M. Burgers
Institute for Fluid Dynamics and
Applied Mathematics
University of Maryland
College Park, Maryland 20742

Professor J. R. Weske
Institute for Fluid Dynamics and
Applied Mathematics
University of Maryland
College Park, Maryland 20742

Professor Pai
Institute for Fluid Dynamics and
Applied Mathematics
University of Maryland
College Park, Maryland 20742

NASA Scientific and Technical
Information Facility
Acquisitions Branch (S-AK/DL)
P. O. Box 33
College Park, Maryland 20740

Professor Loren E. Bollinger
The Ohio State University
Box 3113 - University Station
Columbus, Ohio 43210

Professor G. L. von Eschen
Department of Aeronautical and
Astronautical Engineering
Ohio State University
Columbus, Ohio 43210

Computations and Analysis Laboratory
Naval Weapons Laboratory
Dahlgren, Virginia 22448

Technical Library
Naval Weapons Laboratory
Dahlgren, Virginia 22418

Dr. J. Harkness
LTV Research Center
Ling-Temco-Vought Aerospace Corporation
P. O. Box 5907
Dallas, Texas 75222

Mr. Adolf Egli
Ford Motor Company
Engineering and Research Staff
P. O. Box 2053
Dearborn, Michigan 48123

School of Applied Mathematics
Indiana University
Bloomington, Indiana 47401

Commander
Boston Naval Shipyard
Boston, Massachusetts 02129

Director
Office of Naval Research Branch Office
495 Summer Street
Boston, Massachusetts 02210

Professor M. S. Uberoi
Department of Aeronautical Engineering
University of Colorado
Boulder, Colorado 80303

Technical Library
Naval Applied Science Laboratory
Building 1, Code 222
Flushing & Washington Avenues
Brooklyn, New York 11251

Professor J. J. Foody
Chairman, Engineering Department
State University of New York
Maritime College
Bronx, New York 10465

Mr. F. Dell'Amico
Cornell Aeronautical Laboratory
P. O. Box 235
Buffalo, New York 14221

Professor G. Birkhoff
Department of Mathematics
Harvard University
Cambridge, Massachusetts 02138

Professor B. Budiansky
Department of Mechanical Engineering
School of Applied Sciences
Harvard University
Cambridge, Massachusetts 02138

Dr. Ira Dyer
Bolt, Beranek and Newman, Inc.
50 Moulton Street
Cambridge, Massachusetts 02138

Department of Naval Architecture
and Marine Engineering
Massachusetts Institute of Technology
Cambridge, Massachusetts 02139

Professor Patrick Leehey
Department of Naval Architecture and
Marine Engineering
Massachusetts Institute of Technology
Cambridge, Massachusetts 02139

Professor E. Mollo-Christensen
Department of Aeronautics and Astronautics
Massachusetts Institute of Technology
Cambridge, Massachusetts 02139

Professor A. T. Ippen
Department of Civil Engineering
Massachusetts Institute of Technology
Cambridge, Massachusetts 02139

Professor C. C. Lin
Department of Mathematics
Massachusetts Institute of Technology
Cambridge, Massachusetts 02139

Professor H. C. Hottel
Department of Chemical Engineering
Massachusetts Institute of Technology
Cambridge, Massachusetts 02139

Commanding Officer
NROTC and Naval Administrative Unit
Massachusetts Institute of Technology
Cambridge, Massachusetts 02139

Professor R. F. Probst
Department of Mechanical Engineering
Massachusetts Institute of Technology
Cambridge, Massachusetts 02139

Technical Library
Webb Institute of Naval Architecture
Glen Cove, Long Island, New York 11542

Library, MS185
NASA Langley Research Center
Langley Station
Hampton, Virginia 23365

Dr. B. N. Pridmore Brown
Northrop Corporation
Norair-Division
Hawthorne, California 90250

Dr. J. P. Breslin
Davidson Laboratory
Stevens Institute of Technology
Hoboken, New Jersey 07030

Mr. D. Savitsky
Davidson Laboratory
Stevens Institute of Technology
Hoboken, New Jersey 07030

Mr. S. Tsakonas
Davidson Laboratory
Stevens Institute of Technology
Hoboken, New Jersey 07030

Professor J. F. Kennedy, Director
Iowa Institute of Hydraulic Research
University of Iowa
Iowa City, Iowa 52240

Professor L. Landweber
Iowa Institute of Hydraulic Research
University of Iowa
Iowa City, Iowa 52240

Professor John R. Glover
Iowa Institute of Hydraulic Research
University of Iowa
Iowa City, Iowa 52240

Professor E. L. Resler
Graduate School of Aeronautical
Engineering
Cornell University
Ithaca, New York 14851

Technical Library
Scripps Institution of Oceanography
University of California
La Jolla, California 92037

Professor S. R. Keim
University of California
Institute of Marine Resources
P. O. Box 109
La Jolla, California 92038

Dr. B. Sternlicht
Mechanical Technology Incorporated
968 Albany-Shaker Road
Latham, New York 12110

Mr. P. Eisenberg
HYDRONAUTICS, Incorporated
Pindell School Road
Howard County, Laurel, Maryland 20810

Technical Library
Charleston Naval Shipyard
Naval Base
Charleston, South Carolina 29408

Director
Office of Naval Research Branch Office
219 South Dearborn Street
Chicago, Illinois 60604

Technical Library
Puget Sound Naval Shipyard
Bremerton, Washington 98314

Technical Library
Annapolis Division
Naval Ship Research & Development Center
Annapolis, Maryland 21402

Code ESD-AROD
Army Research Office
Box CM, Duke Station
Durham, North Carolina 27706

Professor Ali Bulent Cambel
Chairman, Department of Mechanical
Engineering
Northwestern University
Evanston, Illinois 60201

Professor A. Charnes
The Technological Institute
Northwestern University
Evanston, Illinois 60201

Barbara Spence Technical Library
AVCO-Everett Research Laboratory
2385 Revere Beach Parkway
Everett, Massachusetts 02149

Dr. Martin Bloom
Director of Dynamics Research
Department of Aerospace Engineering
and Applied Mechanics
Polytechnic Institute of Brooklyn-
Graduate Center
Route 110
Farmingdale, New York 11201

Professor J. E. Cermak
Professor-in-Charge, Fluid Mechanics
Program
College of Engineering
Colorado State University
Fort Collins, Colorado 80521

Mr. Seymour Edelberg
Lincoln Laboratory
Massachusetts Institute of Technology
P. O. Box 73
Lexington, Massachusetts 02173

Technical Library
Long Beach Naval Shipyard
Long Beach, California 90801

Professor A. F. Charwat
Department of Engineering
University of California
Los Angeles, California 90024

Professor R. W. Leonard
University of California
Los Angeles, California 90024

Professor John Laufer
Department of Aerospace Engineering
University Park
University of California
Los Angeles, California 90007

Professor J. F. Ripkin
St. Anthony Falls Hydraulic Laboratory
University of Minnesota
Minneapolis, Minnesota 55414

Lorenz G. Straub Library
St. Anthony Falls Hydraulic Laboratory
University of Minnesota
Minneapolis, Minnesota 55414

Library
Naval Postgraduate School
Monterey, California 93940

Professor A. B. Metzner
Department of Chemical Engineering
University of Delaware
Newark, Delaware 19711

Technical Library
Navy Underwater Sound Laboratory
Port Trumbull
New London, Connecticut 06320

Technical Library
Naval Underwater Weapons Research
and Engineering Station
Newport, Rhode Island 02840

Professor W. J. Pierson, Jr.
Department of Meteorology and
Oceanography
New York University
University Heights
New York, New York 10405

Professor J. J. Stoker
Courant Institute of Mathematical
Sciences
New York University
251 Mercer Street
New York, New York 10003

Engineering Societies Library
345 East 47th Street
New York, New York 10017

Office of Naval Research
New York Area Office
207 W. 24th Street
New York, New York 10011

Commanding Officer
Office of Naval Research Branch Office
Box 39, FPO, New York 09510 (25)

Professor A. G. Strandhagen
Department of Engineering, Mechanics
University of Notre Dame
Notre Dame, Indiana 46556

Miss O. M. Leach, Librarian
National Research Council
Aeronautical Library
Montreal Road
Ottawa 7, Canada

Lockheed Missiles and Space Company
Technical Information Center
3251 Hanover Street
Palo Alto, California 94301

Professor M. S. Plesset
Engineering Science Department
California Institute of Technology
Pasadena, California 91109

Professor H. W. Liepmann
Department of Aeronautics
California Institute of Technology
Pasadena, California 91109

Dr. Jack W. Hoyt (Code P2501)
Associate Head, Ocean Technology
Department
Naval Undersea Warfare Center
3202 E. Foothill Blvd.
Pasadena, California 91107

Dr. F. R. Hama
Jet Propulsion Laboratory
4800 Oak Grove Drive
Pasadena, California 91103

Professor T. Y. Wu
Division of Engineering
California Institute of Technology
Pasadena, California 91109

Professor A. J. Acosta
Department of Mechanical Engineering
California Institute of Technology
Pasadena, California 91109

Director
Office of Naval Research Branch Office
1030 E. Green Street
Pasadena, California 91101

Professor F. Zwicky
Department of Physics
California Institute of Technology
Pasadena, California 91109

Dr. E. E. Sechler
Executive Officer for Aeronautics
California Institute of Technology
Pasadena, California 91109

Dr. R. H. Kraichnan
Dublin, New Hampshire 03444

Technical Library (Code 249b)
Philadelphia Naval Shipyard
Philadelphia, Pennsylvania 19112

Dr. Sinclair M. Scala
Space Sciences Laboratory
General Electric Company
P. O. Box 8555
Philadelphia, Pennsylvania 19101

Dr. Paul Kaplan
Oceanics, Inc.
Technical Industrial Park
Plainview, L. I., New York 11803

Technical Library
Naval Missile Center
Point Mugu, California 93041

Technical Library
Portsmouth Naval Shipyard
Portsmouth, New Hampshire 03801

Technical Library
Norfolk Naval Shipyard
Portsmouth, Virginia 23709

Professor G. W. Duvall
Department of Physics
Washington State University
Pullman, Washington 99164

Chief, Document Section
Redstone Scientific Information Center
Army Missile Command
Redstone Arsenal, Alabama 35809

Professor M. Lessen, Head
Department of Mechanical Engineering
University of Rochester
College of Engineering, River
Campus Station
Rochester, New York 14627

Dr. H. N. Abramson
Southwest Research Institute
8500 Culebra Road
San Antonio, Texas 78228

Editor
Applied Mechanics Review
Southwest Research Institute
8500 Culebra Road
San Antonio, Texas 78206

Dr. S. L. Zieberg, Head
Gas Dynamics Section, Fluid Mechanics
Building B-1, Room 1320
Aerospace Corporation
San Bernardino, California 92402

Mr. Myles B. Berg
Aerospace Corporation
P. O. Box 1308
San Bernardino, California 92402

Mr. W. B. Barkley
General Dynamics Corporation
Electric Boat Division
Marine Technology Center, P. O. Box 911
San Diego, California 92112

Library (128-000)
CONVAIR - Division of General Dynamics
P. O. Box 12009
San Diego, California 92112

Technical Library
Pearl Harbor Naval Shipyard
Box 400, FPO, San Francisco 96610

Technical Library, Code H245C-3
Hunters Point Division
San Francisco Bay Naval Shipyard
San Francisco, California 94135

Office of Naval Research San Francisco
Area Office
1076 Mission Street
San Francisco, California 94103

Gail T. Flesher - 44
GM Defense Research Laboratory
Box T
Santa Barbara, California 93102

Library
The RAND Corporation
1700 Main Street
Santa Monica, California 90401

Dr. H. T. Nagamatsu
General Electric Company
Research and Development Center K-1
P. O. Box 8
Schenectady, New York 12301

Fenton Kennedy Document Library
The Johns Hopkins University
Applied Physics Laboratory
8621 Georgia Avenue
Silver Spring, Maryland 20910

Chief, Library Division
Naval Ordnance Laboratory
White Oak
Silver Spring, Maryland 20910

Dr. R. E. Wilson
Associate Technical Director
(Aeroballistics)
Naval Ordnance Laboratory
White Oak
Silver Spring, Maryland 20910

Aerophysics Division
Naval Ordnance Laboratory
White Oak
Silver Spring, Maryland 20910

Dr. A. E. Seigel
Naval Ordnance Laboratory
White Oak
Silver Spring, Maryland 20910

Dr. S. Kline
Mechanical Engineering 501 G
Stanford University
Stanford, California 94305

Engineering Library
Department 218, Building 101
McDonnell Aircraft Corporation
P. O. Box 516
St. Louis, Missouri 63166

Mr. R. W. Kermeen
Lockheed Missiles & Space Company
Department 57101, Building 150
Sunnyvale, California 94086

Professor S. Eskinazi
Department of Mechanical Engineering
Syracuse University
Syracuse, New York 13210

Professor J. Foa
Department of Aeronautical Engineering
Rensselaer Polytechnic Institute
Troy, New York 12180

Professor R. C. DiPrima
Department of Mathematics
Rensselaer Polytechnic Institute
Troy, New York 12180

Professor L. M. Milne-Thomson
Mathematics Department
University of Arizona
Tucson, Arizona 85721

Dr. E. J. Skudrzyk
Ordnance Research Laboratory
Pennsylvania State University
University Park, Pennsylvania 16801

Dr. M. Sevik
Ordnance Research Laboratory
Pennsylvania State University
University Park, Pennsylvania 16801

Dr. G. F. Wislicenus
Ordnance Research Laboratory
Pennsylvania State University
University Park, Pennsylvania 16801

Dr. A. S. Iberall, President
General Technical Services, Inc.
8794 West Chester Pike
Upper Darby, Pennsylvania 19082

Dr. J. M. Robertson
Department of theoretical and
Applied Mechanics
University of Illinois
Urbana, Illinois 61803

Shipyards Technical Library
Code 130L7, Building 746
San Francisco Bay Naval Shipyard
Vallejo, California 94592

Commander
Naval Ship Research and Development Center
Attn: Code 513 (1)
Code 901 (1)
Code 942 (1)
Code 01 (Dr. Powell) (1)
Code 042 (1)
Code 520 (1)
Code 800 (1)
Washington, D. C. 20007

Commander
Naval Ship System Command
Attn: Technical Library (2052) (1)
Washington, D. C. 20360

Director, Engineering Science Division
National Sciences Foundation
Washington, D. C. 20550

Chief of Naval Research
Department of the Navy
Attn: Code 438 (3)
Code 461 (1)
Code 463 (1)
Code 468 (1)
Code 421 (1)
Washington, D. C. 20360

Commander
Naval Air Systems Command
Department of the Navy
Attn: Code AIR 370 (1)
Code AIR 6042 (1)
Washington, D. C. 20360

Librarian Station 5-2
Coast Guard Headquarters
1300 E Street, N. W.
Washington, D. C. 20226

Division of Engineering
Maritime Administration
441 G Street, N. W.
Washington, D. C. 20235

Commander
Naval Oceanographic Office
Washington, D. C. 20390

Code 2027 (6)
Naval Research Laboratory
Washington, D. C. 20390

Science and Technology Division
Library of Congress
Washington, D. C. 20540

Commander
Naval Ordnance Systems Command
Attn: ORD 913 (Library) (1)
ORD 035 (1)
Washington, D. C. 20360

Library
National Bureau of Standards
Washington, D. C. 20234

Chief of Research and Development
Office of Chief of Staff
Department of the Army
The Pentagon, Washington, D. C. 20310

Dr. Frank Lane
General Applied Science Laboratory
Merrick and Stewart Avenues
Westbury, Long Island, New York 11590

Director
Woods Hole Oceanographic Institute
Woods Hole, Massachusetts 02543

Mr. W. J. Mykytow
AF Flight Dynamics Laboratory
Wright-Patterson Air Force Base
Ohio 45433

Dr. H. Cohen
IBM Research Center
P. O. Box 218
Yorktown Heights, New York 10598